EXPERIMENTAL STUDY OF HELIUM DIFFUSION IN THE WAKE OF A CIRCULAR CYLINDER AT M = 5.8

Thesis by

William Mohlenhoff

In Partial Fulfillment of the Requirements

For the Degree of

Aeronautical Engineer

California Institute of Technology

Pasadena, California

1960

ACKNOWLEDGMENTS

The author wishes to express a sense of deep gratitude to Professor Lester Lees and Doctor Toshi Kubota, who provided expert guidance throughout the subject investigation with frequent and stimulating discussions of the work. Sincere thanks are also extended to Captain M. D. Coffin, USAF, for basic suggestions and the use of his thermal conductivity equipment and to Mr. John McCarthy for his assistance and the use of his total pressure apparatus. Mr. Paul Baloga and the staff of the hypersonic laboratory were very helpful in the installation of the equipment and the conduct of the experiments. Mrs. Betty Laue was very efficient and helpful in the computational phases of the investigation. Mrs. Betty Wood and Mrs. Nell Kindig very skillfully prepared the figures. Special appreciation is also expressed to Mrs. Geraldine Van Gieson for her assistance in the typing of the manuscript.

ABSTRACT

An experimental study of the diffusion of helium in the wake of a circular cylinder was conducted in the GALCIT hypersonic wind tunnel at a Mach number of 5.8. The cylinder was constructed of material having random porosity and was mounted with its axis perpendicular to the stream. The light gas was injected in small amounts and the thermal conductivity method was utilized to detect the concentration of helium in the air at points downstream. Problems in the utilization of the thermal conductivity method for low sample densities were overcome by suitable calibration.

Flow in the wake of the cylinder was found to display characteristically similar behavior at a few diameters downstream, with respect to decay and spread of the concentration. Reynolds number similarity was established in the laminar case, but turbulent Reynolds number similarity may require reference to momentum thickness, which was not possible with the present data.

Profile data was somewhat marred by a tunnel pressure perturbation, but many of the important conclusions were not affected. The profiles appear to follow the theoretical Gaussian distribution in the similar region.

The thermal conductivity method is quite promising as a means of tracing the diffusion of one binary gas constituent in another, as applied to hypersonic wind tunnel experiment. It will also serve in the analysis of transition and turbulence, and of the lateral spreading of the turbulent fluid into the rest of the wake region behind the bow shock.

TABLE OF CONTENTS

PART PAGE

LIST OF TABLES

LIST OF FIGURES

LIST OF SYMBOLS

a	speed of sound
b	cylinder span
A, B	constants
c, C	constants
C_v, C_p	specific heats at constant volume and pressure, respectively
$(C_D)_w$	drag coefficient based on wake dimensions
D	cylinder diameter
D_k	general diffusion coefficient
D_{12}	binary diffusion coefficient
D_T	turbulent eddy diffusion coefficient
f	a function
I	electrical current
K	concentration of helium by mass
K_m	thermal conductivity of mixture
L	a characteristic length
m	mass
$\dot{m}$	mass flow, mass/time
$M_{(\ )}$	molecular weight, (with subscript)
M	Mach number, u/a
p	static pressure
P	total pressure
$\dot{q}$	heat flow, heat energy/time
R	electrical resistance
R	gas constant = $R_o/M_{(\ )}$

R_o	universal gas constant
Re	Reynolds number $= \frac{\rho_e u_e L}{\mu_e}$
t	time
T	temperature
u	local axial velocity
U	test section velocity
V	volume
x	tunnel axis coordinate, positive aft from cylinder center
y	vertical coordinate measured from model center
Y	transformation coordinate $= \int_o^y (\rho/\rho_e)\, dy$
z	model spanwise coordinate
γ	ratio of specific heats, C_p/C_v
δ	characteristic chamber dimension
δ_K	breadth of concentration wake
Δ	denotes an incremental quantity
η	similarity variable $= \frac{y}{\sqrt{D(x - x_o)}}$
μ	absolute viscosity
ν	kinematic viscosity $= \mu/\rho$
ρ	density
σ	standard deviation of normal (Gaussian) curve

Subscripts

a	refers to air
bs	refers to barometric pressure in thermal conductivity cell sample cavity

br	refers to barometric pressure in cell reference cavity
c	refers to conductivity cell chamber quantity
e	external flow quantity, or refers to cell wire ends
g	refers to gas quantity
He	refers to helium
m	refers to mixture quantity
N_2	refers to nitrogen
o	refers to reservoir or initial conditions
p	refers to pitot quantity
s	refers to conductivity cell sample cavity
w	refers to resistance wires of conductivity bridge

I. INTRODUCTION

The problem of the wake behind a blunt body is one of the oldest in the classical, incompressible aerodynamic literature. The practical aspects have centered around the effects of wake vorticity and circulation and the momentum defect determination of drag[1]*. A limited quantity of this classical literature has been directly concerned with the problems of mass diffusion in the wake. There exists, however, a great amount of theory and experimental data on jet mixing of incompressible flows and lower Mach number compressible flows. The jet mixing theory is of course directly analogous to wake theory in many respects, especially in the subsonic case[2]. Also, for the viscous-temperature effects of primary interest here, namely those of the diffusion of momentum, mass and energy, the jets and wakes are just free boundary cases of boundary layer flow for which there is extensive treatment in the literature[3].

A summary of the mixing theory and list of references to 1954 has been contributed by Pai[2]. This compilation indicates that the knowledge of diffusion processes of incompressible flow is fairly complete, and consists for the most part in consideration of momentum-vorticity diffusion. The compressible subsonic theory is also well established, with the addition of some topics of heat energy diffusion. More recent contributions which are of particular interest in the present investigation are the works of Townsend[4], and Schubauer and Tchen[5]. Townsend proposes such ideas as that of the intermittency at outer boundaries of turbulent flows and discusses the wake behind a two-dimensional

---

* Superscripts denote references at the end of the text.

cylinder at some length. Schubauer and Tchen collect and extend the ideas of Townsend and others in a well-integrated description of such flows, and include an excellent bibliography of the associated literature. An additional recent contribution to the specific field of interest here is the book by Hinze[6].

Literature on the supersonic diffusion processes in wakes cannot depend so heavily on the jet mixing literature, and very little has been done, even recently, in this more specific field. Also, the literature described indicates little concern with mass addition and chemical reactions, which have recently become highly important in the hypersonic, high altitude flight regimes of advanced weapon design and space exploration. A number of theoretical and experimental papers have been written in recent years which have demonstrated clearly the importance of these physical-chemical considerations in the transfer of heat to bodies in high Mach number flow media[7-15]. A good summary of associated work is given by Lees[7]. Rubesin[12] and McMahon[13], in particular, show that a light gas is most effective with respect to weight of material injected in reducing heat transfer rates. One concludes from such a literature survey that many hypersonic problems of practical nature will involve the injection of materials in light gaseous state into the boundary layer for cooling, which in turn may result in chemical reactions and nonuniform mixtures of gases in the wake flow behind the body. Any complete study of the hypersonic wake must consider these phenomena.

The wake flow behind a hypersonic body involves the usual considerations regarding afterbodies, structure, and control surfaces, but it has other implications as well which may become quite important. There is, for instance, the probable radar reflectivity and optical

emission properties of the material in the wake, which are of interest in the study of meteor wakes and in the tracking of reentry vehicles, in addition to other obvious military considerations. (Dr. Feldman and his associates at AVCO Research Laboratories are currently investigating these problems.) On the other hand, the study of the hypersonic wake is of current interest as a part of the present exhaustive investigation of the hypersonic flow field in general.

The above considerations have led to the establishment at GALCIT of a program for systematic study of the hypersonic wake behind blunt bodies. Wake pressure measurements at a nominal Mach number of 5.8 have been undertaken by J. M. McCarthy, and temperature and hot-wire anemometry measurements are being conducted by A. Demetriades and C. F. Dewey. In a separate study, M. D. Coffin is continuing the work of McMahon[13] in the investigation of heat transfer with mass injection at the stagnation point of a blunt body. In his work, Coffin has developed an apparatus for the analysis of the concentration of one gas in another by the method of thermal conductivity. The method was known to him through his contact with the work of Rush and Forstall[16], and Forstall and Shapiro[17], at the Massachusetts Institute of Technology.

The present investigation was suggested by Captain Coffin (USAF) and Professor Lees, as a means of extending the GALCIT wake program by a diffusion study. The use of a tracer gas should help in understanding the chemical aspects of wake flow and diffusion in a binary mixture of gases. It was also envisioned that a light gas might be used as a tracer to determine turbulent processes in the wake. Although the thermal conductivity method is a classical one in gas analysis[18], it has seen very little employment in the field of wind tunnel experiment.

In view of some of the limitations of other devices in the usual hypersonic wind tunnel apparatus for the measurement of the physical state of the gas, it has become evident that new methods for obtaining and correlating this type of data are required. A large portion of the discussion below will necessarily involve the setting down of simple procedures, corrections and considerations that have been found essential in the employment of the apparatus. It is hoped that inclusion of all relevant procedures will assist future investigators in avoiding the many small technical delays that interfere with a smoothly conducted experiment. Some improvements to the equipment which could not be incorporated in the present study will also be indicated.

Thus, the present investigation is a study of the effectiveness of the thermal conductivity method for determining concentration of a tracer gas. At the same time it is an exploratory study of the utility of this tracer gas in uncovering the nature of hypersonic wakes behind blunt bodies.

II. EQUIPMENT AND PROCEDURE

II. 1. General Experimental Method

In accordance with the cited objectives the following experimental steps were planned:

(1) Ejection of light gas from a porous body of simple geometric shape at a nominal Mach number of 5.8 in carefully controlled small quantities.

(2) The extraction of samples of the wake at various stations in the tunnel by means of a small pitot tube. These samples were to be led to a thermal conductivity cell which would compare concentration of the diffusing agent in the sample with a known reference gas. This procedure requires a calibration of the thermal conductivity of known mixtures of the two gases against cell readings.

(3) The correction of the data for mean tunnel concentration, differences in pressure of the sample and reference cell, instrument errors, and any other effect that might alter consistency and reproducibility of the readings from test to test.

(4) The comparison of wake pressure data taken for the ejection model against that of the solid model used for total head surveys, (McCarthy's model), to correlate results.

(5) Experimental check of the two-dimensionality of the tunnel flow at the center of the model, and spanwise uniformity of the tracer gas ejection.

(6) The reduction of the data to find what conditions of similarity may be found in the flow, and whether turbulent zones can in fact be defined by the method.

(7) The comparison with available theory and related experiment.

II. 2. Selection of Diffusion Gas

The selection of a tracer gas for diffusion into the tunnel air that would best meet the requirements of the experiment was simple. If one checks the list of the common unobjectionable, relatively inexpensive laboratory gases, helium and hydrogen are the two most suited to the application and most sensitive to thermal conductivity measurement. Helium is 5.97 and hydrogen 7.15 times as conductive as air, but hydrogen is inflammable[16]. (See Table 1.) The choice of helium becomes obvious, and it is certainly one of the light materials that might be employed in surface cooling applications. The commercial helium utilized was 99.9976 per cent pure, with traces of carbon dioxide, argon, hydrogen, nitrogen, and methane, by typical analysis.

II. 3. Description of the Wind Tunnel

The GALCIT hypersonic wind tunnel is a closed return, continuously operating tunnel with two test section legs. The legs are designed to be used alternately to provide for installation in one while the other is operating. Leg 1 has nozzle blocks set for a nominal Mach number of 5.8 in the 5" x 5.25" x 29" test rhombus. The leg 1 operating limits are as follows: reservoir pressure, P_o = -5 to 100 psig; reservoir temperature, T_o = 225 to 325°F; for which Reynolds number per inch, $Re = 3.88 \times 10^4$ to 30.3×10^4. The Reynolds number per unit length is obtained by the formula

$$Re/L = (P_o/\mu_o)\ M \sqrt{\frac{\gamma}{(\gamma - 1)\, C_v\, T_o}}\ (T_o/T)^{\frac{\gamma-2}{\gamma-1}}\ \frac{\frac{T}{T_o} + \frac{198.6}{T_o}}{1 + \frac{198.6}{T_o}}\ , \quad (1a)$$

for a perfect gas, where zero subscripts refer to reservoir quantities, isentropic expansion from P_o is assumed, and the equation for the variation of viscosity with temperature is the Sutherland formula:

$$\frac{\mu}{\mu_o} = \frac{T_o + 198.6}{T + 198.6}\,(T/T_o)^{3/2} \quad . \quad (2)$$

For these tests with M = 5.8 and T_o = 275°F:

$$Re/in = 2260 \times P_o \quad , \quad (1b)$$

where P_o is measured in psia. The velocity of the test section flow at this nominal Mach number and T_o is U = 2770 ft./sec. as computed by the formula:

$$(U/a_o)^2 = \frac{2}{(2/M^2) + (\gamma - 1)} \quad ; \quad a_o = \sqrt{\gamma R T_o} \quad , \quad (3)$$

where a_o is the reservoir speed of sound[22]. The reservoir pressure could be varied between approximately 0 - 100 psig, but critical starting and running conditions were avoided by limitations of 10 - 85 psig.

A more complete description of the tunnel and compressor plant is to be found in References 19 and 20. A schematic drawing of the tunnel is included in Figure 1 and of the test section and related experimental equipment in Figure 2.

II. 4. Model Construction and Installation

The basic model of the GALCIT hypersonic wake study at present is the two-dimensional circular cylinder. The body geometry was purposefully kept as elementary as possible in order to simplify the correlation of data. Once the complete flow field for this model is established the experimental methods for the simple model can be extended and applied to more complex shapes. It was found that a 0.3" cylinder diameter was the maximum that could be employed for consistent starting of the tunnel flow. Thus, a .3" x 5" cylinder was mounted horizontally from wall to wall in the forward part of the 5 inch wide tunnel test section (Figure 2). Initially the model was installed at a point 13.2" aft of the nozzle throat. In the later tests, however, the model was moved an additional 2.6" aft to obtain better flow conditions. (See the discussion in Section III.)

McCarthy's total head and static pressure surveys were being made with a brass model. Although brass might be made porous, it was thought that a more suitable material should be found with a surface as smooth as possible and with natural random porosity. These properties were found in an alumina refractory rod of the type used to support furnace heater elements. The refractory rods initially were of .385 inch exterior diameter and 0.13 inch interior diameter. The exterior of the model was carefully turned to a smooth, uniform .3 inch diameter, but the interior diameter could be as much as .003 inch non-concentric, because of warping of the rod. The slight non-symmetry of helium flow that would result from this interior eccentricity was considered of negligible concern as to its effect on wake measurements of gas concentration,

in view of other experimental difficulties that appeared to exclude such minor considerations at the time of model selection. Unfortunately, the rod material was somewhat brittle and the models had to be replaced frequently because of breakage. In spite of these deficiencies of the alumina rod the material was considered well suited to the present application, because it provided low, well distributed helium flow rates with low metering pressure during bench tests. Thus, the momentum of the ejected gas is small for a given mass flow, and should not appreciably alter the external flow and shock wave structure. It was desirable to achieve this result, if possible, in order to correlate diffusion data with the pressure data of McCarthy's experiments as directly as possible, and therefore obviate the necessity of duplicating a large amount of his work.

The bench tests of the models mentioned above included other considerations which are peculiar to this experiment. First, it was noted during preliminary tunnel runs that a light-surface coating of oil would collect on the model surface. The oil problem is a continuing difficulty in the GALCIT tunnel for which a satisfactory solution could not yet be found. It was therefore necessary to measure in some way the effect of the oil on the flow of helium through the rod surface. After several hours of running, the lightly oil-coated side of the rod was covered and the model was connected to a vacuum pump at one end, with the other end sealed. The difference in the amount of vacuum the pump would draw against a sealed space, and against the uncovered side of the model, was measured with a U-tube manometer. The oil coated side showed a negligible change in porosity. The oil problem therefore was not considered serious, since the model could be rotated from test to

test to collect an even distribution of oil, and the flow level could be adjusted to provide the same flow of helium regardless of slight changes in model porosity.

One must also make certain that all the metered helium is ejected through the cylinder and not lost in faulty seals at the tunnel walls. A clamping and locking arrangement and soft "o"-rings were installed to prevent such leakage. After each installation the vacuum test described above was applied to determine if the seal was consistently good. The helium was injected from both ends of the model in order to provide a more uniform flow distribution across the cylinder span. The model was mounted between metal ports because of the difficulty of securing an injection model in glass ports when the installation must be repeatedly disassembled. Schlieren studies were therefore not feasible with the cylinder injecting helium. However, comparison of the flow characteristics with and without helium flow could be obtained by taking representative total head pressure traverses.

II. 5. Control of Helium Injection

The flow of helium entering the cylinder at the tunnel walls was metered with a standard Fisher-Porter Tri-flat flowrator, (Tube No. 3-F-3/8-25-5/70, having a 3/8 inch glass ball), in series combination with a smaller Fisher-Porter flowmeter (Tube No. OIN-15, 1/8 inch steel ball). The large flowrator provided stable measurement of the flow in spite of "back-pressure" variances of the model, while the small flowmeter provided a double check and a more sensitive, vernier-type monitoring of the flow quantity. The metering pressure was maintained by reference to a standard U-tube mercury manometer. (See Figure 2.)

Although the temperature correction is small, the temperature of metering was noted for each test.

The metering of helium through the flowmeters was checked against the Fisher-Porter Company predictions and the previous laboratory calibrations for helium flow. This calibration was accomplished by the timed displacement of a large volume of water at several helium flow rates. The large flowrator checked closely with the manufacturer's prediction, but the smaller flowrator was affected too seriously by back-pressure of the water to accomplish a good test. The flow of helium was therefore always based on the reading of the large flowmeter, with the smaller meter as a check against variances in cylinder porosity by the back pressure effect. The test was conclusive to about $\pm$ 3.5 per cent accuracy in the flow range of interest, which is also approximately the order of accuracy in setting of the flow for the tunnel experiments.

II. 6. Sampling Probe

The probe employed to withdraw flow samples from the wake of the injection model was of the type designed for total pressure measurements in boundary layers. The tip was constructed by compressing a hypodermic tube to a flat orifice of 0.004" depth with 0.039" width. The tip was faired out to a 0.25" O. D. stainless steel tube fitted with a 0.067" I. D. neoprene tubing at the downstream end for transport to the gas analysis cell. The same probe was used for total head traverses in the wake.

The probe was mounted in a mechanism designed to traverse it axially from zero to 27 model diameters aft of the model centerline, and

vertically 1.2" upward to 2.0" below the axial centerline of the tunnel. The probe could be set to an accuracy of about 0.01" axially and 0.001" vertically. (See Figure 2.)

Samples were withdrawn despite the low pressure of the tunnel by the creation of a near vacuum condition in the conductivity cell. (This procedure will be explained in more detail in the next section.) In the case of the lower tunnel pressures (near the model and at lower reservoir pressure) a relatively slow time constant for gathering of the sample was noted - on the order of 30 seconds. It was considered essential to utilize the small probe, however, because of the narrow regions of helium distribution to be encountered near the model.

II. 7. Thermal Conductivity Apparatus and Procedures

The thermal conductivity or heat transfer capacity of a gas mixture is a distinct physical quantity that may be used in various ways to detect, identify and trace the concentration of one binary constituent in another. A very comprehensive summary of the principles and some of the more common applications is presented by Daynes[18]. An application in which helium was traced is the work of Rush, Forstall, and Shapiro[16,17], where the method was utilized to trace diffusion in coaxial gas jets at low speed. The form of the equipment in the present experiment is similar to that designed by Rush and Forstall. It was designed by M. D. Coffin at the GALCIT hypersonic laboratory.

The thermal conductivity method of comparing two gas mixtures consists fundamentally in passing the mixtures in question through identical cell chambers with electrical resistance elements forming legs of a Wheatstone bridge. (See cell diagram, Figure 3, and wiring diagram,

Figure 4.) The resistance elements in the two chambers have equal currents since the resistances are paired in the two legs of each chamber. Small variances can be removed by adjustment of the dividing resistance at the bridge input. When the gas conductivity in one chamber equals that in the other, the wire heat, (I^2R), is conducted through the walls of the chamber, in equal amounts for the two chambers, and a balance is achieved with no voltage across the bridge. The resistance of the wires in the two chambers is not varied other than by the chamber temperatures. Also, in the bridge, one holds the current constant and essentially measures a change in R, the resistance of sample chamber wires. Thus $R = R(T_w)$, where T_w is the wire temperature. T_w is dependent on wire heat loss by the energy balance,

$$\dot{q}_w = \dot{q}_g + \dot{q}_e = I^2R \quad ,$$

where neglecting radiation and in stagnant gas:

$\dot{q}_g$ = heat loss through the gas = $K_m(\Delta T/\delta)$

$\Delta T = T_w - T_c$, the difference between wire and chamber wall temperature

δ = typical chamber dimension

$\dot{q}_e$ = heat loss through wire ends = $C\,\Delta T$, where C = coefficient of wire conductivity times wire area, in appropriate units.

Then

$$I^2R = \left(\frac{K_m}{\delta} + C \right) (T_w - T_c) \quad . \tag{4}$$

The chamber walls conduct rapidly enough to assume T_c = constant. (In this case the chamber walls were constructed of brass.) With constant current Eq. (4) then gives a relation between R, K_m, and T_w. The mixture conductivity, however, is a function of concentration of the

mixture species and the temperature, T_m, of the mixture, by the kinetic theory relations (Cf. Reference 2, page 159). The mixture temperature of the combination of helium and air can be expressed as some function of ΔT, or as approximately the mean, $\overline{T}_m = (T_w - T_c)/2$. One can thus replace K_m in Eq. (4) by the above equation from kinetic theory and then T_w by a linear function of R, arriving at

$$R = R_o + \Delta R = f(K_o + \Delta K) \quad . \tag{5}$$

Thus, each Wheatstone bridge resistance, R, is a function only of the change in concentration of the helium in an air-helium mixture surrounding it. In this case, the bridge resistance in the cell cavity containing helium enriched air is reduced by the greater cooling capacity of the light gas. The variation of resistance in one chamber will cause a voltage unbalance across the bridge which can be read on a sensitive potentiometer. Equation (5) can best be evaluated in terms of this potential for purposes of calibration by laboratory measurement of known sample concentrations. (See Section II. 7. 1.) Other schemes of operation are feasible, but this method is one of the most adaptable to this experiment and was especially convenient in that a commercially manufactured cell could be utilized. (The specifications and manufacturer of the particular cell chosen are given in Figure 3.)

Although the fundamental procedures outlined above are conceptually simple, several additional problems arose in procuring representative samples from hypersonic flow fields, and in removing possible sources of error from the method. These are the considerations which determine specific design of the apparatus and operating procedure, and which will be discussed in succeeding paragraphs.

They can be classified under the following headings:

(1) proper calibration of the cell

(2) adequate handling of the sample

(3) pressure differences between the two chambers

(4) temperature difference effects

(5) instrument errors and accuracy.

(An additional item of consideration here might be the handling of dissimilar mass flows between the two chambers. However, since hypersonic tunnel samples are widely variable in density and large errors would be introduced by convective cooling effects, it was decided from the outset to stagnate both sample and reference gases.) The above five items will be discussed in turn with regard to how they affected the design and/or procedure of the experiment.

II. 7. 1. Cell Calibration

The calibration curve of potential across the bridge versus concentration of helium in a reference gas must be obtained by a laboratory method, as shown in conjunction with Eq. (5). The reference gas used must be one which remains consistent in heat conductivity after calibration for each subsequent filling of the reference chamber. In this case, if one were to employ room air in the reference chamber, filling the chamber for each period of use, an error may be introduced by departure from the calibration curve because of changes in the atmospheric mixture. The air mixture may change with small percentage variations of carbon dioxide and water vapor. The carbon dioxide variation will not be significant, but water vapor partial pressure is sufficiently variable and water vapor is sufficiently different in thermal

conductivity that noticeable error may be introduced if dry air is not used. (See Table I.) Since the air in the hypersonic tunnel is well dried and otherwise sufficiently uniform in content from one test period to the next, a sample of helium-free tunnel air was taken as the reference gas before each test.

Having selected the reference gas as tunnel air, the cell calibration should be made with air-helium mixtures against dry air. The collection of large quantities of tunnel air is inconvenient, however, and the present calibration procedure involved the comparison of known mixtures of helium in dry nitrogen with pure nitrogen. Since the conductivity of nitrogen is very close to that of air, this procedure involves an error of smaller magnitude than that of preparation of the known mixtures and plotting and reading of the graph. The magnitude of the error involved can be estimated by noting that nitrogen is 0.996 as conductive as air, (Table I). Thus, an error on the order of one part in 250, or .4 per cent, is the result of comparing any sample against a reference of nitrogen instead of dry air. The difference in concentration obtained between comparison of a sample containing large quantities of nitrogen against a nitrogen reference and comparison of a similar air-helium sample against air is therefore quite negligible.

The samples were prepared by allowing a bottle of high pressure nitrogen to discharge into a bottle of helium, with a sensitive gage measuring the pressure of the helium bottle accurately before and after the addition of the nitrogen. The partial pressures of the two gases in the volume then determined the concentration of the mixture. The preparation was therefore independent of possible nitrogen leakage during the transfer. The method of computing the concentrations is

based on the equation of state for components of a perfect gas mixture:

$$p_{He} = \rho_{He} R_{He} T_m = (M_{He}/V_m)(R_o/M_{He}) T_m \quad ,$$

where

p_{He} = partial pressure of He, measured before mixing

R_o = universal gas constant

M_{He} = molecular weight of He

V_m = mixture volume, constant

T_m = mixture temperature, constant

m_{He} = mass of helium

$p_2 = p_{N_2} + p_{He}$ = pressure measured after mixing, by Dalton's law.

Solving for m_{He} ,

$$m_{He} = \frac{p_{He} V_m M_{He}}{R_o T_m} \quad .$$

Similarly,

$$m_{N_2} = \frac{p_{N_2} V_m M_{N_2}}{R_o T_m}$$ is the mass of nitrogen.

Thus

$$K_{He} = \frac{m_{He}}{m_{He} + m_{N_2}} = \frac{p_{He} M_{He}}{p_{N_2} M_{N_2} + p_{He} M_{He}} \quad . \qquad (6)$$

Equation (6) is utilized to obtain the newly mixed concentration. A series of samples was prepared, having different concentrations of He in N_2. As each sample was prepared, its concentration was read in terms of voltage deflection across the thermal conductivity bridge. The plot of these calibration points is a smooth curve with little scatter. (Figure 5).

Temperature and pressure must be equal in the two cell cavities for a proper calibration. (Pressure and temperature are discussed more completely in the sections to follow.) Also the calibration curve is applicable only for the voltage and current utilized across the bridge when the sample deflections were read. The voltage and current choice depend on two conflicting considerations. Calibrations which are more sensitive and linear can be obtained for higher voltage-current combinations, as shown by the curves of Rush and Forstall[16]. On the other hand, it is desirable to keep cell resistance-wires warm by leaving the electric current on while drawing the next sample, in order to minimize the time required for the cell temperature to reach equilibrium in the measurements. However, during the sample collection, the gas density in the chamber becomes very low, and hence the voltage-current combination must be low so that the wires will not produce heat faster than it can be dissipated. (See Sections II. 6. and II. 7. 2.) Even though the current was turned off before gathering a sample, the lowest sample densities are within a few millimeters of the vacuum pressure, when the current must be on to read the bridge deflection. It is therefore necessary to calibrate the cell with the lowest satisfactory power to prevent fusing of the hot wires. To accomplish the sensitivity adjustment in this case, a variable resistance across the potentiometer terminals is utilized. (See Figure 4.) For calibration over the low concentration range of interest in the experiment, a current of 80 milli-amps with a 3 volt dry-cell circuit was employed, and the potentiometer resistance was set so that an essentially linear curve was obtained in the 0 - 2 per cent range. (See Figure 5 for equations of portions of the curve.)

II. 7. 2. Sampling Equipment and Procedure

The method of obtaining a representative gas sample from the hypersonic tunnel is somewhat more critical than in other applications because of the low pressures encountered (on the order of one millimeter of mercury). An intermittent sampling system is required in order to stagnate both sample and reference for proper comparison.

As previously mentioned, the reference air was drawn from the tunnel in the present experiment prior to commencement of the helium flow. The bridge was balanced with the dry tunnel air in both sample and reference cavities. Samples were withdrawn, after the helium flow was commenced, by creating a near vacuum at the outlet of the cell (Valve 3, Figure 2). In order to compress the sample as much as possible to compare it properly with the reference air taken at atmospheric pressure, a hand-operated mercury pump was included between the tunnel and conductivity cell. The pump in this case had a compression ratio of about three to one. The pump included a U-tube pressure scale, accurate to about 1 mm of mercury. Referring to Figure 2, valves 1, 2, and 3 are sequentially opened and closed with a continuously operating vacuum pump so that the sampling steps are accomplished as follows:

(1) evacuation of the cell, mercury pump, and connecting lines

(2) washing of the new sample through the same volumes

(3) re-evacuation of the volumes, which establishes a vacuum in the cell

(4) drawing of sample with valve 3 closed, and the mercury flask lowered

(5) Compressing of the sample with valve 1 and 3 closed. The time required for each of the above steps is a function of the sample density. A low density sample enters the cell slowly because of low pressure differential between cell vacuum and probe total head. It is important to determine the proper time interval for each step. The time of taking one sample point is generally 3-4 minutes at best by this procedure, but if it is hurried the sample may not be representative. The time for each step is found by taking an extended time at first, and then reducing the interval until a discrepancy is noticed in comparison with the same sample point taken over a longer time interval. This time interval is most critical for the lowest sample pressures.

The sampling apparatus was thoroughly leak-checked prior to each test run by applying low vacuum to the mercury pump, tubing and cell cavities, closing the valves, and noting whether or not the vacuum is maintained by the mercury column. Even a slight leakage of room air into the system would cause gross contamination of the sample. Also, when a known sample is put in the sample cavity and left overnight, the same reading could be read again before the next test period, as a simple day to day check.

Another pertinent remark should be made in regard to the method of collecting the reference sample. Since the pressure calibration depends on the difference between the cell cavities, one should be careful to see that the reference sample is collected at exactly atmospheric pressure. This objective may be accomplished by proper sequencing of the valves at the time of collection, (i. e., shutting of the entrance valve an instant before the exit valve). Once the reference sample is collected at a known barometric pressure, it need not be changed again

during the test period.

II. 7. 3. Pressure Difference Calibration

The application of the thermal conductivity method of gas analysis to hypersonic flow requires some suitable means of correction for differences in pressure between the sample and reference cavities of the conductivity cell. For slight pressure differences this error is negligible, but when the reference gas is at atmospheric pressure and the sample at a few millimeters of mercury absolute, the error in neglecting the pressure difference may amount to 50 per cent or more of the concentration reading taken. Simple kinetic theory predicts that the heat conductivity coefficient of a gas is independent of pressure if the mean free path of the gas molecules is much less than the chamber dimensions, and proportional to pressure in the opposite limiting case. The transition from one limiting case to the other is shown experimentally by Bomelburg[23]. His graph of heat loss versus Knudsen number (proportional to pressure) clearly indicates a smooth transition from the independent region to the proportional region at Knudsen numbers corresponding to the low pressures of the hypersonic wind tunnel, if the chamber dimensions are such as to permit such a transition. It was evident from the experiment by Bomelburg and from a few preliminary tests that the pressure correction to conductivity would be required in the present investigation.

It is not simple, mechanically, to pump a representative sample from the wind tunnel at near vacuum to a pressure of one atmosphere in the sample chamber. Most methods of accomplishing this compression involve the use of a pumping fluid medium which may contaminate the

sample. While it is certainly desirable to investigate such means extensively, a simple expedient to circumvent the need for such a pump is to calibrate the error in bridge potential against the corresponding pressure difference. This calibration is accomplished by reading the bridge deflection of a known concentration sample at reduced pressures. The sample potential is initially checked at one atmosphere and then a portion removed in steps by a vacuum pump until very low pressures are reached. The new potential across the conductivity bridge is read for each step. A suitable means of plotting the resulting calibration curve for correction of tests is evident by physical reasoning, supported by experiments like that of Bomelburg[23]. One is led to the conclusion that the conductivity of the gas in each cell cavity, and therefore any unbalance of the bridge, is a function of the absolute pressure in the cavity, when the pressure is low enough that wall effects begin to become important. Thus, if

p_s = pressure in sample cavity, cm. Hg. absolute

p_{b_s} = barometric pressure of the open end of the U-tube column measuring pressure in the sample cavity, cm. Hg., a slowly varying function of time

p_{b_r} = barometric pressure, p_{b_s}, of the room at the time when the reference gas is collected, cm. Hg.

Δp = height of mercury column, cm.

Then

$$p_s = p_{b_s} - \Delta p$$

is the independent variable in a function which determines the emf error due to low pressure. Now $p_{b_s} \cong p_{b_r}$ for any given calibration or test where the barometer does not change more than a few mm of Hg., as is invariably the case. The emf correction is not detectable on the

instruments when the sample and reference cells are so nearly equal in pressure. One can thus say that $p_{b_r} = p_{b_s}$ so far as conductivity in the cell is concerned. To provide for barometer fluctuations, the absolute pressure of the sample cavity should be plotted in atmospheres as

$$(p_s/p_{b_s}) = (p_{b_s} - \Delta p)/p_{b_s} = 1 - (\Delta p/p_{b_s}) \quad ,$$

for the abscissa of the calibration plot. The graph of Figure 6 is the result of the calibration. The points fall closely along the same curve for the three low concentrations utilized. Tunnel air reference points cannot be distinguished from nitrogen versus helium-nitrogen points in the small scatter at higher pressure differences. The scatter is the result of instrument inaccuracies, sampling variances, and the pressure measurement inaccuracy of the mercury pump scale. The pressure measurement was accurate to about 1 mm of mercury. Redesign and construction for better accuracy was not considered essential in this initial wake survey, in view of other experimental inaccuracies of the same order of magnitude. Also, only a few points near the model involve pressure calibration at the very low pressures. A maximum of ten per cent inaccuracy for the pressure calibration at very low pressures was accepted in that it would normally involve much less than ten per cent error in the total readings of bridge potential. The corresponding percentage error for any concentration level may be obtained from Figure 6. The scatter in the lower concentration region of the curve is entirely the result of slight variances in the sample and instruments used at the time of the calibration. The emf correction here is small, and the best average of the points was taken in the curve fairing. (Later, the potentiometer was replaced and the micro-ammeter improved in order

that less scatter would be obtained in taking the wake concentration surveys. See the instrument discussion in the next section.)

The pressure calibration certainly would show a variation with concentration if the concentrations were of a higher magnitude than the 3 - 5 per cent levels measured in this investigation. A series of pressure difference curves with various concentration levels as a parameter would be required for high concentrations.

It is well to note that a pressure calibration for one geometry of the apparatus might not be the same as for another where the dimensions of the tubing and cavity were changed. This would be the result of mean free path and cell hot wire end loss effects. (These effects are discussed in the literature of kinetic theory and hot wire anemometry, Cf. Reference 22.)

Finally, the following list of steps is given for a careful and precise pressure correction of the type that would be required for emf accuracies of 97 - 98 per cent with the lowest sample pressures to be found near the model at $M = 5.8$:

(1) measurement of sample pressures in the range of 1 - 20 mm of mercury absolute to an accuracy of 0.1 mm, and higher pressures to 1 mm

(2) accurate calibration curves for known sample concentrations

(3) collection of reference gas at a known (atmospheric) pressure

(4) monitoring of barometric pressure throughout the test

(5) computation of pressure differences between cell cavities and normalization by the barometric pressure. (Since the variation in barometric pressure may be as much as 3 - 4 mm of mercury for a test run of several hours, each critical

reading can be computed using a curve of barometric pressure for the times of the test.)

The alternative to this procedure is the pumping of each sample to atmospheric pressure in the sample cavity with no contamination during the process. In the present test, the above five steps were applied as closely as possible, within the 1 mm accuracy of the mercury pump pressure scale, and with special care during the critical readings.

II. 7. 4. Temperature Difference Effects

Normal variances in room temperature will not affect the accuracy of the thermal conductivity bridge as long as the temperature is equalized between the sample and reference cell cavities. (This was shown by Eq. (5) above, and its derivation.) This statement can be made as long as the temperature coefficient of conduction for the gases to be compared is approximately equal. This factor determines the variation of heat conductivity with temperature, and is nearly the same for the gases considered here (Table I). The protection from radiating devices and stray air currents in the room by a wooden container and the use of high heat conductive brass for the cell material, help to insure the equalization of temperature. The brass also provides some equalization between cell cavities for samples brought in at a temperature unequal to the room temperature of the reference cell. The sample traverses a distance of 3 or 4 feet in the room and is compressed in the mercury pump; also, there is a finite time between sample collection and reading of the bridge. The temperature of the average sample therefore cannot be greatly different from the room temperature of the reference cell. It is well, however, to estimate the effect of a small

temperature difference in the bridge deflection reading. This estimate has been accomplished by Daynes[18], who states that the simple precautions given above are quite adequate to prevent serious effect of temperature differences between cell cavities. One may, however, install the cell in a thermostatically controlled housing if very accurate readings of low conductivity differentials are desired.

Daynes, in his book, has given a very extensive coverage of the more obscure considerations in the method of thermal conductivity gas analysis. He includes such factors as vibration and other secondary effects. His conclusions regarding the detection of highly conductive gases in air, however, are that very small concentrations can be measured with accuracy if only the precautionary measures of the present experiment are employed.

II. 7. 5. Control of Instrument Errors

Referring to Figure 2 the instruments employed for measurement of the concentration potential difference were

(1) the milli-ammeter

(2) the thermal conductivity cell

(3) the precision potentiometer with its associated standard cell and galvanometer (The galvanometer is utilized to obtain a null current through the potentiometer circuit.).

A simple method for control of most of the possible errors in these instruments was available through the employment of the samples prepared for the calibration procedure. A sample was put in the sample cavity before each test run and the bridge emf was checked. The ratio of the calibrated value to the present emf was then a corrective factor for the

readings of the bridge during the test. This procedure also served to correct for variations in room temperature, as a check on the bias setting of the bridge sensitivity, and as a check for damage or contamination of the conductivity cell. Along with a standard cell comparison, it also served to check the performance of the potentiometer. Carefully mixed samples of known concentration are therefore indispensable in the use of the thermal conductivity method. Frequently, as mentioned in the sample leakage control discussion above, the known sample was left in the cell for extended periods of time and the same reading was obtained upon recheck. The reproducibility of such readings on known samples was within about one per cent at all times.

The bridge was balanced by a null indication on the galvanometer and potentiometer before each test with the dividing resistance at the bridge input, (B+, Figure 4). This balance was accomplished with nitrogen in reference and sample cavities, and then with air in both as a recheck while gathering the tunnel reference air before injection of helium. The stability of the cell zero potential was within 0.05 m.v. at all times.

II.8. Total Pressure Apparatus and Procedures

The magnitudes of injected helium concentration to be measured in a flow depend inversely on the local density and velocity of the flow. The determination of these quantities at any station of interest is therefore mandatory to a complete understanding of the diffusion processes. It is not an easy matter to obtain such quantities in a compressible flow[22]. The total and static pressures are relatively easy to obtain, but the measurement of another state variable is

required to determine density and velocity. The additional measurements might be the speed of sound, the temperature, or the direct measurement of velocity and density, if these measurements were feasible and dependable. At present, methods for close determination of these flow variables are not fully reliable. One may assume isoenergetic flow, however, without serious error in first order calculations, and compute an approximate local temperature. The pressures are then measured with suitably designed probes and associated manometers or transducers, after which the Mach number can be obtained through the Rayleigh pitot relation[22]

$$p/p_{o_2} = \frac{\left(\frac{2\gamma}{\gamma+1} M_1^2 - \frac{\gamma-1}{\gamma+1}\right)^{1/(\gamma-1)}}{\left(\frac{\gamma+1}{2} M_1^2\right)^{\frac{\gamma}{\gamma-1}}} , \qquad (7)$$

where

p = static pressure

p_{o_2} = total pressure behind probe normal shock wave

M_1 = Mach number ahead of probe shock wave

γ = ratio of specific heats.

The Mach number and pressures may then be employed to determine other fluid quantities.

As previously mentioned, a pressure study by J. McCarthy in the wake of a 0.3 inch brass cylinder was also in progress at the time of the present experiment. It was desirable in terms of wind tunnel running time to utilize the pressure data from the brass model in the diffusion studies made with the porous model. This procedure required a comparison of the two models as to flow characteristics, without

injection and with helium injection at the level to be metered during the wake diffusion tests. The total pressure profiles were considered the best means of comparison. Total pressure profiles behind the injection model were therefore made with the equipment employed by McCarthy. This equipment will be described more completely in his report, but a brief description will be given here.

The probe utilized in the total head traverses behind the cylinders was the same instrument employed to gather diffusion samples, and was described in Section II. 6. The total pressure in the probe was first read with a mercury micro-manometer at one or two points in the flow, after the tunnel had been stabilized at the test reservoir conditions. The total pressure was then diverted to a Statham 1 psi differential pressure transducer with a reference pressure provided by a silicon oil column. The transducer converted the pressure to electrical potential which was traced on a Mosely xy- plotter. The transducer-plotter system was calibrated by measuring the pressure with the mercury micromanometer at a few points. The output from a voltage divider coupled to the probe traversing mechanism was fed into the x- scale of the plotter. Sufficient additional micro-manometer points were read to establish that the recorder scale had not shifted during the tunnel traverse. All pressures were referred to a very low vacuum and therefore were plotted as absolute pressures. The micromanometer pressures were non-dimensionalized with the tunnel reservoir pressure converted to absolute units before making the traverse. Thus, the pressure traverses are plotted in a convenient form for comparison of flow characteristics.

McCarthy had also taken static pressure traverses of the wake behind the brass cylinder. A comparison of static pressures with the porous model, however, was considered unnecessary in that total head profiles would give sufficient insight into any flow differences, which should not be large.

Results of the wake studies depend greatly on whether two dimensional flow actually existed in the tunnel across the cylinder span. A few representative total head traverses were therefore made to check the two dimensionality of the flow approximately one inch from the tunnel centerline.

II. 9. Correction and Correlation of Data

The reduction of emf data from the conductivity bridge requires a certain sequence of steps according to the discussion concerning the several items of equipment in the preceding sections. Before outlining the reduction technique, however, it will be necessary to show how the build-up of helium in the tunnel circuit may affect the data.

The quantity of helium in the tunnel air can be predicted by a brief analysis. Helium concentration does not build up in value indefinitely, but approaches an asymptotic ratio of helium mass to tunnel air mass which is dependent on the amount of make-up air added to the tunnel circuit and the corresponding leakage rate from the circuit. The governing equations are analogous to those for water vapor in the tunnel air, where the amount of water vapor is controlled by the bypassing of circuit air for drying to prevent condensation in the test section. The equation for the tunnel helium concentration can be derived as follows:

Let $\dot{m}_{He}$ = constant mass/time of He entering the tunnel

$\dot{m}_a$ = constant mass/time of make-up air entering the tunnel

M = mass of mixture in the tunnel,

K = concentration by mass of He in the mixture

$\dot{m}$ = mass of mixture leaving the tunnel with concentration K, which must equal the total mass entering for steady tunnel operation, or

$$\dot{m} = \dot{m}_{He} + \dot{m}_a = \text{a constant} \quad .$$

Therefore, the rate of change of helium concentration is given by

$$dK/dt = \frac{\dot{m}_{He} - (\dot{m}_{He} + \dot{m}_a) K}{M} \quad .$$

The solution of this equation with $K = 0$ at $t = 0$ is as follows:

$$K = \frac{\dot{m}_{He}}{\dot{m}_{He} + \dot{m}_a} \left[1 - \exp\left(- \frac{(\dot{m}_{He} + \dot{m}_a)}{M} \; t \right) \right] \qquad (8)$$

Equation (8) demonstrates that the tunnel concentration tends to an asymptotic constant value as t becomes sufficiently large. This result was confirmed experimentally in preliminary tests. Within the accuracy of the thermal conductivity measurement, the time required to reach a constant value was on the order of 10 - 15 minutes for the normal quantity of make-up air, $\dot{m}_a$, utilized to replenish the tunnel circuit. The tunnel concentration with normal make-up air and low reservoir pressure is of the same order of magnitude as the lower concentration readings. It is therefore desirable that as much as possible of the background concentration be removed. Make-up air was increased to accomplish this removal by excess leakage until levels of helium concentration about .06 per cent or less were obtained at the several reservoir pressures.

Equation (8) shows that the asymptotic constant value of tunnel

concentration reached is independent of tunnel P_o, and is dependent only on the rate of helium and air added to the tunnel. (The rapidity in reaching the asymptotic value, however, is dependent on P_o through the tunnel cycle mass of air, M.) This result was also shown to be correct when the valves admitting make-up air were left fixed and the tunnel P_o was changed for some of the tests. When the mass rate of the helium and the corresponding tunnel concentration are known, the make-up air rate can be computed by Eq. (8). If the make-up air rate is too high the tunnel air will not be sufficiently dried, and errors in measurement of helium concentration may be introduced through lowering of the air conductivity by water vapor. The tunnel concentration may vary during a test if the make-up air is changed. It was therefore checked at intervals and corrections were made as necessary in the data reduction.

Perhaps the best method of discussing the reduction of concentration test data is to follow a typical data sheet (Table II) and reduction sheet (Table III). The values of concentration in millivolts read for a series of distances, y, from the vertical centerline are entered in the reduction sheet, along with the corresponding pressure differences, Δp, between the current atmospheric pressure and the sample cavity pressure. The computation is started in column 6 with the subtraction of the tunnel background concentration from the emf reading. The tunnel concentration sample is always compressed to atmospheric pressure, which allows subtraction before Δp correction. The computation is continued with column 7, where the emf reading of the conductivity bridge is corrected for instrument errors by the ratio of the emf of a known sample to its current reading. (The instrument correction is not large, for it can be controlled by the variable resistance across the potentiometer terminals.) This ratio corrects for variations in current measurement, room temperature,

and slight change in cell characteristics as discussed in previous sections.

Column 9 of Table III scales the Δp vacuum versus barometric pressure reading of the mercury column to that barometric pressure. The barometric pressure taken at one time during the experiment is sufficiently accurate unless very low tunnel densities are expected. If these densities are such that the ratio $\Delta p/p_{bs} > .99$, it is well to take into account shifts in barometric pressure of greater than 1 mm. Fortunately such low pressures are found only very close to the model in restricted regions, where the concentration is normally high. The percentage error is therefore low in the total emf reading for a relatively high error in Δemf caused by cell cavity pressure differences.

The $\Delta p/p_{bs}$ value is utilized in Figure 6 to obtain the Δemf correction for column 10 of Table III. Finally the emf versus concentration graph of Figure 5 is entered to obtain the concentration, K, in per cent of helium by mass.

The remaining step before plotting of the concentration data is the determination of the centerline from the maximum concentration point. This step is carried out after the Δp correction has been applied in order to determine the true maximum. In some of the tests only enough points were taken vertically above and below the centerline to determine the true maximum for rate of decay versus axial downstream distance. If a profile were somewhat skewed, the centerline was determined by equal spacing of half-maximum points. (This point will be covered in more detail in the later discussion.)

The helium flow for some of the early tests was not exactly the 0.0031 lb/min of the later tests. It was changed after the profile runs

to improve the exactness of the setting. A scale factor of 1.15 was applied to the data of the early runs to refer all runs to the same helium flow. The linearity of such a correction for small ranges is shown by Figure 7, which is a plot of a few points taken at different helium flow rates with the probe fixed at an arbitrary location behind the model. This procedure would be in error if the concentrations measured were not in the linear portion of the millivolt versus per cent calibration curve, Figure 5.

Finally, before proceeding to the results of the experiment, an estimate should be made of the errors to be expected in the concentration data produced by the equipment and procedures employed. The types and causes of the errors have been covered to a great extent in the above discussion. A more complete summary of them is included in Table IV, with an estimate of magnitudes wherever possible. This table may serve as a guide to improvement of the accuracy of the method. A fairly complete reference concerning accuracy of thermal conductivity measurement is the book by Daynes[18].

II. 10. Summary of Test Parameter Variations and Test Objectives

In view of the simplicity of the apparatus in the present exploratory investigation and the resultant long time intervals required in the measurement of individual wake samples, the number of parameters to be varied in the tests was held to a minimum consistent with the basic objectives previously cited. The most important parameter in the wake flow processes of interest is of course the Reynolds number. Variation of Reynolds number was achieved by holding the reservoir temperature

at $T_o = 275^oF$ and altering the tunnel reservoir pressure alone, according to Eq. 1b. (Reynolds numbers of the tests are included in Table V.) The helium ejection rate was held at a constant low nominal value of .0031 lb/min throughout the tests. This was ascertained to be the flow quantity desirable for proper tracing of the processes with minimum effect on the momentum of the basic flow.

The investigation, with the above considerations, included the following tests:

(1) Determination of the maximum concentrations behind the model for representative axial distances to the limits of probe travel (27 diameters) for supply pressures P_o = 10, 35, 60, 85 psig, and all other conditions held constant. The maximum concentration would be determined by taking three or four samples near the tunnel centerline until the maximum is well defined. These tests were required to determine how the maximum concentration decays with axial distance behind the model.

(2) Measurement of flow samples for concentration at a sufficient number of points off the vertical centerline to determine a concentration profile at various downstream stations. These traverses for a number of such stations would then display conditions of spreading and regions of similarity in the flow. The combination of centerline maximum concentration points taken and the profiles should then determine regions of turbulent flow. To restrict the amount of tunnel operating time, the profile traverses were limited to the extreme pressures considered, P_o = 10 and 85 psig.

(3) Total pressure traverses were planned at a representative

downstream distance, $x/D = 5$, for the supply pressures P_o = 10, 35, 60, and 85 psig, with and without helium injection. Comparison with data from the brass model would then show corrections that should be made for pressure differences, in utilization of that data for the porous model.

(4) Total pressure traverses were to be taken off centerline to determine if the flow is two-dimensional at a representative station, $x/D = 5$ for P_o = 10 and 85 psig.

(5) Monitoring of the flow at intervals during the concentration runs was also to be included, by the taking of sufficient total head traverses to see if conditions in the flow field remained consistent.

These were considered the minimal tests that could be made to determine a satisfactory general description of the flow and diffusion processes affecting the injected helium. From such a limited investigation, then, a much more extensive survey could be planned, with improved equipment and technique for coverage in reduced tunnel operating time.

Each test was designed to duplicate points of a previous test to check for repeatability of helium flow setting, model installation characteristics, conductivity apparatus variations, and possible alteration of the basic flow. Correlation of such repeated data would then establish a confidence level and accuracy check of the procedures.

A typical data sheet for the recording of concentration test data is included as Table II. The fixed parameters are included in the sheet, and the remaining blanks are explained by the discussion of the previous sections.

III. RESULTS AND DISCUSSION

III. 1. General Discussion of the Flow

At hypersonic speeds the flow field around a blunt body is dominated by the bow shock (Figures 8, 9). The static pressure on the front portion of a circular cylinder with its axis perpendicular to such a stream is much greater than ambient pressure, and the pressure falls steadily along the surface. When the boundary layer is laminar, flow separation occurs some distance aft of the position of maximum thickness (Figures 8, 9). The static pressure along the inclined free shear layer is very nearly constant and this layer is nearly straight until just upstream of the characteristic "neck" formed in the wake. Then the flow deflects and the pressure rises abruptly in a short distance, while the flow velocity in the wake cavity along the dividing "zero" streamline is brought to rest. A second shock wave is produced by this flow deflection. This oblique wave is intercepted by the expansion fan generated at the body surface and decays rapidly in the downstream direction.

When the free shear layer is laminar the width of the "neck" is of the same order as the boundary layer thickness at the separation point on the body. In the Reynolds number range of the present experiment, the cylinder boundary layer is laminar at separation, which is confirmed by the fact that the neck is extremely narrow in comparison to the body diameter. Rapid lateral diffusion of vorticity and heat takes place as the fluid moves downstream. Of course, the gradients of enthalpy and velocity in the "external" flow which has traversed the bow shock are also being smoothed out by laminar diffusion, but the time scale of this process is

several orders of magnitude longer.

If a foreign gas is ejected from the surface of the circular cylinder it will also be concentrated at the narrow "neck", provided the free shear layer is laminar. Downstream of the neck, the lateral diffusion of this tracer gas furnishes a measure of the efficiency of the laminar mixing process. At sufficiently high Reynolds numbers, transition to turbulent flow is observed to occur in this inner wake downstream of the neck. The subsequent lateral diffusion of the tracer gas in this case gives some insight into the rate of spreading of the turbulence into the "external" flow field. Of course the problem is complicated near the neck, but further downstream the lateral concentration profiles should exhibit a certain similarity. Consider a point far enough downstream of the neck so that $u_e - u << u_e$. Then the Oseen approximation can be employed, and the diffusion equation to this approximation is as follows:

$$\rho u_e (\partial K/\partial x) = (\partial/\partial y)\left(\rho D_K \frac{\partial K}{\partial y} \right) \quad , \tag{9}$$

where $D_K = D_{12}$, the binary diffusion coefficient for laminar flow, and $D_K = D_T$, the turbulent eddy diffusion coefficient for turbulent flow. For laminar flow one absorbs the density into the Howarth-Dorodnitzyn variable by letting

$$Y = \int_0^y (\rho/\rho_e)\, dy \quad .$$

By utilizing the approximation

$$\rho(\rho D_{12}) = \text{constant} = C \rho_e^{\,2} (D_{12})_e$$

as analogous to the usual $\rho\mu$ = constant for the velocity defect solution, Eq. (9) is reduced to the form:

$$\partial K/\partial x = \frac{C(D_{12})_e}{u_e} \frac{\partial^2 K}{\partial Y^2} \quad . \tag{10}$$

In addition there is the condition for the conservation of the tracer gas, namely,

$$\dot{m} = \int_{-\infty}^{\infty} \rho\, u\, K\, dy = \text{constant}, \tag{11a}$$

or

$$\dot{m} \cong \rho_e\, u_e \int_{-\infty}^{\infty} K\, dY = \text{constant} \quad . \tag{11b}$$

The solution to Eq. (10) with the condition given by Eqs. (11a) and (11b) is the well-known Gaussian distribution

$$K = \frac{A}{\sqrt{C(D_{12})_e\,(x/u_e)}} \exp\left(- \frac{Y^2}{4(D_{12})_e\, C\,(x/u_e)} \right), \tag{12}$$

where

$$A = A_1 \quad (\dot{m}/\rho_e u_e) \quad , \quad (A_1 = \text{a constant}) ;$$

i. e.,

$$K = A_1 \frac{\dot{m}}{\sqrt{C\,\rho_e^{\,2}\,(D_{12})_e\, u_e x}} \exp\left(- \frac{Y^2}{4(D_{12})_e\, C(x/u_e)} \right). \tag{13}$$

The conclusions indicated by this first order laminar solution are that

(a) $K_{max} \sim 1/\sqrt{x}$, given p_e , $\dot{m}$;

(b) Since $(D_{12})_e \sim \nu_e \sim (\mu_e/\rho_e)$,

$K_{max} \sim 1/\sqrt{p_e}$, given x, $\dot{m}$;

(c) $K/K_{max} = \exp\left(- \frac{Y^2}{4(D_{12})_e\, C(x/u_e)} \right)$,

indicating the Gaussian shape of the concentration profile.

Now for turbulent flow the situation is more complicated because

the turbulent eddy diffusion coefficient is not independent of axial distance. Roughly speaking, $D_T = B\Delta u\, \delta_K$, where Δu is the velocity difference across the turbulent inner wake, B = a constant, and δ_K is the breadth of the inner wake. As the turbulent fluid penetrates into the "external flow", D_T increases. Nevertheless a first approximation for the turbulent case is obtained by regarding D_T as a constant. Making another first order approximation, let $\rho = \bar{\rho}$, a mean value in Eq. (9). Then the lateral concentration profile for the turbulent case is similar to the laminar solution, except that $(D_{12})_e$ is replaced by D_T, Y is replaced by y, and C = 1 in Eq. (13). Now

$$D_T/u_e = \frac{B(C_D)_w D}{4} \quad ,$$

where $(C_D)_w$ is the drag coefficient associated with the momentum defect of the turbulent inner wake and D is the cylinder diameter. Then for turbulent flow:

$$K = A_2 \left(\frac{\dot{m}}{\rho_e u_e D}\right) \frac{1}{\sqrt{\frac{B C_{D_w}}{4}}} \frac{1}{\sqrt{x/D}} \exp\left(-\frac{y^2}{B C_{D_w} Dx}\right) . \quad (14)$$

The conclusions drawn from the first order "solution" of the turbulent case are that

(a) $K_{max} \sim 1/\sqrt{x}$, given p_e, $\dot{m}$, C_{D_w} ;

(b) $K_{max} \sim 1/p_e$, given x/D, $\dot{m}$, C_{D_w} ;

(c) The profile of K/K_{max} is Gaussian.

Before examining the experimental data in the light of the preceding rough similarity considerations, certain flow conditions

discovered during the tests must first be discussed.

III. 2. Tunnel Flow Conditions and Variations

During the course of the pressure traverse tests made with the brass model and the concentration tests with the porous model, certain discrepancies began to appear. (Both models were mounted in the same tunnel position, 13.2 inches from the nozzle throat.) Discrepancies were first seen in the pressure data taken by McCarthy, prior to the concentration runs. (See Table VI.) In particular, it was noted that reproducibility of the pressure traces was not good, and that square-shaped and non-symmetrical wakes were being obtained. Actually, Gaussian distributions of wake diffusion quantities are to be expected, according to the discussion in Section III. 1. The discrepancies in the pressure traverses were attributed in part to oil droplet formation on the brass model. (It diffused over the surface of the porous model.) However, it was not until a quantity of pressure and concentration data was taken that the discrepancy affected the data seriously enough to be certain that it, in fact, existed. The chronological history of the flow can be followed by referring to Tables VI and VII and the corresponding figures (Figures 10-21), which are the complete presentation of the experimental data obtained. In particular, Figure 13 shows the effect of the flow change in spreading of helium mass; Figure 14 shows the effect on axial decay; and Figures 16-18 are pressure traverses which show the variations in the momentum defect of the wake core. Figure 19 demonstrates that the flow is identical for the two models. Figures 18 and 19 demonstrate that the effect of helium flow is that of a slight lowering of the wake total

pressure, by 5 per cent or less at P_o = 85, and widening of the shocks and wake core at P_o = 10 psig. Density effects of the light gas are undoubtedly the factors which caused these differences in total head traverses.

When all of the above figures are reviewed, one comes to the conclusion that tunnel flow perturbation is certainly evident. A few pressure traverses were taken without the model. These traverses and some calibration history of the tunnel revealed that two small waves originating in the nozzle throat region crossed the tunnel at almost the exact position of the model. Their symmetry had made them impossible to detect in the early data. Their effect was to cause intermittent variation in the pressure of the wake and widening of all the wake total pressure "buckets". This effect can be verified by noting that the pressure traverses taken with the probe off center actually correspond closely to those taken with the model moved rearward 2.6 in. out of the perturbation region. (See Figures 16c, 18b, 18c, and 19b.) These conclusions were confirmed by intermittently taking concentration data and pressure traverses with the model at the rear position until the data of concentration runs 10 - 15 was obtained without another shift of the flow. The runs taken with a stable flow then serve as a means of correlating the previous concentration profile data and obtaining some useful information from it. This procedure is justified only because of the precautions taken in all concentration tests, namely those of repeating sample points from preceding runs to check reproducibility. The small variations in the duplicated points which were noted at the time of taking the profile data could now be understood. Originally, these were attributed to errors in helium flow setting or to instrument errors.

It was considered impractical in this exploratory study to repeat the data of the first runs for the present investigation, after moving the model to the stable position. Rather, it was decided to utilize the data in its present form to extract as much information as possible, and then to repeat and expand the experiment in another investigation, with improved equipment based on the knowledge gained to date. Actually the effect of this compromise on the remaining discussion is not as great as might at first be expected.

III. 3. Continuity Check of Helium Flow

By integrating the diffusion equation to suitable limits of the concentration profile, one obtains

$$\int_{-\delta_K}^{+\delta_K} (\partial/\partial x)(\rho u K)dy + \int_{-\delta_K}^{+\delta_K} (\partial/\partial y)(\rho u K)dy = \int_{-\delta_K}^{+\delta_K} (\partial/\partial y)(\rho D_{12} \frac{\partial K}{\partial y})dy \quad .$$

Since the concentration and concentration gradient in the y- direction are both zero at the wake edges, the integral equation is reduced to

$$(\partial/\partial x) \int_{-\delta_K}^{\delta_K} \rho u K \, dy = 0 \quad ,$$

where the order of differentiation and integration has been interchanged. This result can only be valid if

$$\int_{-\delta_K}^{\delta_K} \rho u K \, dy = \text{constant} = \dot{m}_{He}/\text{ unit length} \quad , \tag{15}$$

which expresses the fact that the mass of helium injected from the cylinder into the stream must equal the integral of the $\rho u K$ profile taken at any station, x , and integrated over the span. Thus if one assumes two-dimensionality of the flow, the integral

$$\int_0^b \int_{-\delta_K}^{\delta_K} \rho u K \, dy \, dz = \dot{m}_{He} \quad , \quad \text{mass/sec} \tag{16}$$

would equal the helium flow quantity metered into the cylinder. The integral provides a means of checking whether or not the concentration measurement is accurate, providing the product ρu can be determined. The method of computation for ρu follows from the equation of state and appropriate modifications:

$$\rho u = p\,(Ma/RT) = pM\sqrt{(\gamma_m/R_m T)} \quad ; \tag{17}$$

where γ_m and R_m are the ratio of specific heats and gas constant of the mixture of helium and air. If the assumption is made that the flow is iso-energetic (with possible error not greater than approximately 10 per cent), the local temperature can be replaced by the well-known relation,

$$T = \frac{T_o}{1 + \frac{\gamma_m - 1}{2} M^2} \quad . \tag{18}$$

The Mach number may be determined from the pressure data taken by McCarthy, which corresponds to the concentration profiles taken before large shifts in the tunnel flow. The method of obtaining the Mach number from this data is given in Section II. 8, for $\gamma = \gamma_m$. Although the static pressure is given only for the wake center, McCarthy has found by taking representative traverses that static pressure is very nearly constant over wake cross-sections between inner shocks downstream of the wake "neck".

To provide greater accuracy in the $\rho u K$ calculation, one should apply a correction to the static pressure for the helium defect in the wake. (See Figures 18 and 19.) A measurement of the static pressure with and without helium flow should ordinarily have been made. It is reasonable,

however, that the velocity is not changed and that the static pressure, p, is changed by the same ratio as the total pressure, $P_p = p + \rho/_2 U^2$, because of the density effect of the helium. The effect in this case was so slight that no correction to p was made. The Mach number does not change in any case, with the assumption that the velocity change is very small.

An accurate computation of the ρuK quantity also requires that the parameters γ_m and R_m be replaced by their true values, rather than by approximating them with $\gamma_a = 1.4$ and $R_a = 1,716$ ft.^{2}/sec^2 ^oR for air, because the parameters of the two binary constituents are quite different in the case of helium and air. ($R_{He} = 12,438$ ft.^{2}/sec^2 ^oR and $\gamma_{He} = 1.667$) The equation for the gas constant is

$$R_m = \sum K_i R_i = KR_{He} + (1 - K) R_{He} \quad , \tag{19a}$$

where K = concentration of helium in air, by mass. The equation for the ratio of specific heats is

$$\gamma_m = \frac{(1-K)\, c_{p_a} + K\, c_{p_{He}}}{(1-K)\, c_{v_a} + K\, c_{v_{He}}} = \frac{(1-K)\gamma_a + K\gamma_{He}\left(\dfrac{c_{v_{He}}}{c_{v_a}}\right)}{1 - K + K\dfrac{c_{v_{He}}}{c_{v_a}}} \quad . \tag{20a}$$

When the numerical values for the gas parameters are substituted, the two equations become

$$R_m = 1,716 + 107.22K \tag{19b}$$

$$\gamma_m = \frac{140 + 5.351K}{100 + 3.350K} \quad . \tag{20b}$$

The value of ρuK obtained for each vertical distance, y, by the above procedure, is plotted as in Figure 23. The integration by planimeter then gives the mass per unit span. The double integration is complete when

the mass/span is multiplied by the span length, b = 5 in. The two example curves of Figure 22 came from the profile data of Figures 10 and 11 and the corresponding pressure and Mach number profiles of Figures 20 and 21. The non-symmetry of the puK profiles is to a certain extent the result of non-symmetry in the total pressure profiles, but may also be caused by the non-uniform injection of helium through the cylinder. Four such integrations were possible with the available data and were completed with the result:

$P_o = 85$	$x/D = 15$	$\dot{m}_{He} = .00279$ lb/min
$P_o = 85$	$x/D = 20$	$\dot{m}_{He} = .00300$ lb/min
$P_o = 10$	$x/D = 9$	$\dot{m}_{He} = .00307$ lb/min
$P_o = 10$	$x/D = 15$	$\dot{m}_{He} = .00281$ lb/min

These values are to be compared with the flowrator setting $\dot{m}_{He} = .00305 \pm .00010$ lb/min. (The second value above was taken by doubling a half-concentration profile, after the flow had shifted slightly.) Even though the several approximations above were made, the values have less than 10 per cent error and 10 per cent spread. It could be argued that the results are somewhat fortuitous, but it is unlikely that gross errors could have cancelled each other for the four different cases at two tunnel reservoir pressures. One is led to the fairly safe conclusion that:

(a) The iso-energetic temperature assumed is within about 10 per cent of the true value.

(b) The static and total pressure measurements are dependable.

(c) The concentration measurements are also to be trusted within the accuracy predicted by Table IV.

(d) The tunnel instability was not serious in this case because

the pressure and concentration profiles corresponded.

(e) Even better accuracy should be obtained if the instrumentation is improved and the model is located in the rear position.

(f) Two dimensional flow is, for all practical purposes, a certainty. (This conclusion is supported by the relatively good agreement between the forward off-center pressure traverses and those taken with the model in the rear position.)

III. 4. Discussion of the Diffusion and Similarity Properties

The values of all maximum concentrations taken at the wake centerline are plotted in Figures 14 and 15. The plot of Figure 14 was included to show the effects of the flow shift on axial decay at P_o = 85 psig, when the model was in the forward position. The points plotted in Figure 15, however, are those taken with stable flow conditions when the model was moved to the rear position. Unfortunately this shift in model position reduced the probe travel behind the model centerline to 27 diameters instead of the previous 36, but by this expedient a complete and consistent set of axial decay points at four P_o values was obtained. The flow was checked before, during, and after the runs by total pressure traverses with the probe at 5 diameters. The stable traverses of Figures 16 - 19 were consistently duplicated. Having established a fairly high degree of confidence in the data of Figure 15 by the continuity check of the previous section and the evidence of stable flow, this plot may be discussed in the light of previous experiment and theory.

When the word similarity is used in the following discussion it should be construed to mean similarity or approximate similarity in the general sense; that is, a scaling of the flow according to certain laws

relating the coordinates and diffusion parameters, such that all cross-section profiles taken at downstream positions have the same structure and shape and follow the same decay rule. Townsend attached this meaning to the term "self-preserving"[4], and reserved the term "similarity" for the more specific Reynolds number similarity in turbulent flow, requiring that the "processes which determine the main structure of turbulent motion are substantially independent of viscosity". This essentially applies to all turbulent free boundary flows in the continuum regimes at high velocity. It does not mean, however, that the boundary conditions of the flow cannot be influenced by viscosity, as indeed they must in the case of the cylinder wake, where the drag coefficient is a function of Reynolds number.

III. 4. 1. Downstream Decay of Maximum Concentration

The theory shows for the present case that the maximum helium concentration should be distributed down the tunnel centerline in inverse proportion to the square root of x , the axial coordinate. Further $K_{max} \sim x^{-\frac{1}{2}}$ should be true of the flow in either the laminar or turbulent case. The plot of Figure 15 indicates that this condition is true in only the P_o = 10 psig case for the region beyond x/D = 4. A constant slope for the other reservoir pressures is indicated, however, for regions sufficiently far downstream. In the physical case, it is realized that the model axis is not necessarily the origin of the similar flow, and that in order to compare the slope of the decay curve with theory, one must determine the virtual origin of the similar flow by a suitable auxiliary plot. This procedure is accomplished for the present data by plotting

the values $1/K_{max}^2$ against the coordinate, x , on a rectangular plot. (See example, Figure 23.) Though scatter is enlarged by this procedure, a straight line through the points is evidently a good approximation to their distribution, showing that the $x^{-\frac{1}{2}}$ condition is satisfactorily met, with virtual origin as indicated by the x-intercept. The resulting correction to the plot of Figure 15 for all four reservoir pressures is included in Figure 24. It can be seen that the maximum concentration does at least closely approximate the decay condition given by the theory.

It should be noted that a few points in Figure 15 fall below the normal scatter of the data. A close check of the experimental data sheets revealed that the points marked in the figure were taken at the end of a day of operation with high tunnel make-up air. It is quite likely that the tunnel drying equipment could not remove sufficient quantities of water vapor in these cases, and the conductivity of the tunnel air was lowered as compared to the reference sample taken at the beginning of the run. With the relative conductivity of water vapor as given in Table I, about 1 per cent by mass would have been sufficient to cause the observed deviations. This is then a likely reason for the appearance of the profile taken at 24 diameters in the P_o = 10 psig case of the early data (Figure 11) which was also taken at the end of a long test period with high make-up air. The use of high make-up air for other than short runs therefore appears questionable. Another expedient would be to collect a reference sample for each tunnel sample, but this would increase the time of taking a reading and the possibility of error in the procedure.

III. 4. 2. Variation of Maximum Concentration with Tunnel Pressure

The separation of all the curves in Figure 24, for the various reservoir pressures, does not appear to be a function of P_o alone, but is dependent on some other condition of the flow. Since the theory calls for $K \sim 1/\sqrt{p_e}$ proportionality at a given x/D in the laminar case, one immediately checks to see if the condition is satisfied in the present data. This is done by checking the slope of the auxilliary plot made to determine the virtual origin, x_o, or by checking the ratio between straight-line portions of the curves in Figure 24. The condition is satisfied for the case of $P_o = 10$ versus $P_o = 35$ psig, with

$$\sqrt{P_o(35)/P_o(10)} = \sqrt{(35 + 14.4)/(10 + 14.4)} = 1.42 \quad ,$$

where 14.4 psi is the average barometric pressure of the laboratory elevation. It is not satisfied for

$$\sqrt{P_o(60)/P_o(35)} \quad \text{or} \quad \sqrt{P_o(85)/P_o(60)} \quad ,$$

where the values for the absolute square root ratio are 1.23 and 1.16, respectively. Furthermore, the flow does not satisfy the predicted condition for the fully turbulent case in either of these comparisons, in that the K_{max} values are not scaled directly by the pressure ratios,

$$P_o(60)/P_o(35) \quad \text{and} \quad P_o(85)/P_o(60) \quad .$$

A possible conclusion indicated by these facts is that the flow at $P_o = 60$ psig is in a region of transition from laminar to turbulent flow and that the flow at $P_o = 85$ psig is fully turbulent. The flows at $P_o = 10$ and 35 psig are of sufficiently low Reynolds number that they are laminar.

These statements are supported by the related pressure traverses which were taken intermittently with the concentration runs to check flow stability (Figures 16 - 18, runs 10 - 13). The wake portion of the pressure traverse in the P_o = 60 psig case is narrower and deeper than that of the P_o = 85 trace. This trend is opposite to that between the P_o = 10 and P_o = 35 psig cases, where the P_o = 10 trace becomes shallower at the wake center on the nondimensional scale, and remains at about the same width. Schlieren photographs and hot-wire studies made by A. Demetriades also support these conclusions. Transition at 3 - 4 diameters in the P_o = 85 case is indicated, and at 4 - 5 diameters in the P_o = 60 psig case. In both cases it appears that the mechanism of transition commences in the 2 diameter region, corresponding to the position of the necked-down portion of the wake. (See Figure 15.) The other possible explanation for the lack of predicted scale between the K_{max} turbulent P_o curves, is that the drag affects the scaling in a manner which cannot be determined by the present data. (The appearance of C_{D_w} in the boundary condition of the turbulent case was shown in Section III. 1.) The present data is inadequate in that momentum thickness could not be properly computed because of the effect of the tunnel perturbation.

III. 4. 3. Transverse Spread of Concentration

The similarity of concentration profile shapes may be checked by plotting the normalized concentrations K/K_{max} versus the normalized y coordinate y_{av}/y_m, where y_{av} is the mean of the positive and negative absolute values and y_m is the same mean taken at the half-maximum point of concentration. The curves are thus fitted at two points and the scatter pattern of the remaining points checked for similarity. The plots

of Figures 25 and 26 are the result of such a procedure. It can be seen that, except for the $x/D = 3$ case at $P_o = 10$, the curves indicate a similarity as to shape of the spreading concentration profile. The exception noted in the $x/D = 3$ curve is to be expected, since it is too close to the origin of the similar region and an anomaly appears in the data of Figure 11. The profile points taken at $P_o = 85$ after a slight shift of the flow, plot equally well with the profiles at 9 and 15 diameters before the flow shift. Having thus established at least reasonable shape similarity and the decay with $x^{-\frac{1}{2}}$, one may plot K/K_{max} versus

$$\eta = \frac{y/D}{\sqrt{(x-x_o)/D}} = \frac{y}{\sqrt{D(x-x_o)}}$$

and obtain one curve for all profiles. This is done for the $P_o = 85$ case in Figure 27, with the appropriate virtual origin for the flow shift. In addition, a mean, $\bar{\eta}$, and standard deviation, σ, are computed from the curve faired through the points, and the two parameters are used to compute a Gaussian distribution for comparison with the faired curve. The mean is just the width of the half-profile base and the standard deviation is given by

$$\sigma^2 = \frac{\sum \eta^2 (K/K_{max})}{\sum (K/K_{max})} - \bar{\eta}^2 ,$$

for discreet values of the abscissa. The chi-squared test of statistical theory could be applied to determine the percentage confidence in the normality of the distribution. It was not done for this case because the tunnel perturbation effect would alter the meaning of the result. Reasonable certainty of agreement with the theory, however, is indicated.

In spite of the tunnel flow difficulties, it can be stated in summary that the flow is approximately similar for $x/D \geq 9$ throughout the Reynolds number range investigated. The related incompressible literature indicates that much greater downstream distance is required for the flow to achieve complete similarity[4]. One possible reason for this difference is that the proper transverse length scale for the hypersonic "inner wake" is actually much smaller than the body diameter, so that a distance of 9 - 10 body diameters corresponds to a distance of many inner wake momentum thicknesses.

III. 4. 4. Non-Similar Regions of the Flow

Very little quantitative evaluation of non-similar flow regions has been presented in the literature. This is understandable in view of the fact that these are regions of rapid adjustment in which nonlinear, fluctuating effects take place in the transition from one state of natural flow to another. In the wake of the hypersonic cylinder, such regions are to be found in the narrow portion of the wake and in the near vacuum at the rear of the model. A typical profile observed in the wedge shaped cavity between the model and the neck of the wake is that of Figure 28. The trapezoidal shape is evident until the concentration profile achieves a triangular distribution at the neck, after which the statistical effects of diffusion alter the shape toward that of the error curve. The base and point of the triangle are last to achieve the characteristic normal distribution in the similar flow downstream. This effect is also observed in the incompressible coaxial jet profiles of Forstall and Shapiro[17]. The trapezoidal region corresponds to their jet potential core.

III. 5. Suggestions for Improvement of the Experimental Method and Scope of the Wake Investigation

III. 5. 1. Improvement of the Apparatus

Several suggestions have previously been made concerning the apparatus, but a few additional points could be made, after reviewing the data obtained.

III. 5. 1. a. Model Construction

The data reveals that porosity of the model was adequate, but improved uniformity would possibly remove some of the unsymmetric behavior of the profiles. A few variations in the flow were noted which are not accounted for by the tunnel perturbation. It is possible that these resulted from model surface condition effects on the drag. The surface conditions are affected by model tool marks and other defects and the oil problem in the tunnel. These factors can be reduced to a minimum if the oil problem can be solved and the same model and model orientation is used for each test. The concentration measurements are very sensitive to drag effects on the wake pressure.

III. 5. 1. b. Probe Installation

The probe is restricted in the present installation to about 27 diameters of travel, after moving the model rearward. The traversing mechanism should be modified to give about 50 - 60 diameters of travel downstream. It should be provided with a positive locking system to prevent shift during measurements, and a micrometer scale. It should be small enough in cross-sectional area to provide easy starting of the

flow. (This was a problem in the present investigation, with a probe mechanism of about 5/8 inch circular cross-section.)

III. 5. 1. c. Helium Flow Metering

The metering of helium flow in the present investigation was satisfactory only after it was realized that model back pressure caused variances in the meter reading for the same mass flow, if the small meter was used. The large meter provided the necessary stability to differences in model porosity, but it was necessary to read the scale very accurately. The reading could be improved by the installation of a light and magnifying glass on the meter, with the provision of a means of sighting the level of the ball through a reticle or gunsight arrangement to insure consistency of eye level. With this arrangement the helium flow could be turned off and on at will and readjusted quickly, which would reduce the usage of helium during periods of apparatus adjustment and check-out.

III. 5. 1. d. Sampling Apparatus and Procedure

There are two major difficulties with the present sampling system that should be corrected before extensive testing is resumed:

(1) The times required to clear the previous sample and bring in a new one are unnecessarily long.

(2) The accuracy of the pressure correction is not satisfactory for very low sample densities.

For the first problem, there are two possible solutions: The first has been previously mentioned as the pumping of each sample to barometric pressure. This method has attendant difficulties with regard

to possible contamination of the sample. In addition it requires a valve sequencing and pumping method which may become complex. It does, however, also eliminate the second problem. The second method is to follow the procedure utilized in the present investigation, measuring the pressure defect after a single compression, but to use larger compression ratio and provide automatic sequencing wherever possible. The automatic sequencing is desirable for precision and alleviation of the natural tendency to allow extra time for each step of the procedure. It could be accomplished by a suitable system of relays and solenoid-operated valves. The time would be even more reduced if a sensitive recorder is used in place of the potentiometer and the pen dropped for each sample point, in the relay sequencing. The proper time constants could be set in the relays with a few preliminary measurements at each reservoir pressure. The system and valves would have to be leak checked, of course, at frequent intervals. A rough diagram of a suitable system is included as an Appendix.

The second problem, of measuring the pressure accurately, can be handled by reading total pressure intermittently with sample readings on the same recorder plot, if the sample is not compressed. Compression is desirable, however, at the very low tunnel densities, to prevent the pressure correction from becoming as large as the sample reading. If a transducer were installed on the sample volume the pressure could still be read intermittently on the recorder, and the total pressure at the probe could also be plotted as a third trace.

The proper combination of the above ideas should provide equipment which would operate to take sample points automatically after each

movement of the probe. The Appendix is an example of one such possible combination. Sample points could be read in times of less than one minute if equipment of this type could be developed, instead of the several minutes average per point required in the tests of the present experiment.

In addition to these problems, the water vapor contamination is of some additional concern. Either high tunnel make up air should be utilized and a reference sample gathered from the tunnel circuit, or low make up air with the single reference sample as taken in the present tests.

III. 5. 1. e. Instrument Specifications

The potentiometer of the present experiment was of Leeds and Northrup manufacture and was sensitive to four decimal places in millivolt units. It was well suited to the tests. Three decimal place accuracy is sufficient, but stability of zero is important. A recorder utilized in place of the potentiometer would need to meet the same specifications.

The ammeter utilized was of the standard laboratory variety, accurate to about one-tenth milli-amp. An accuracy of 0.01 milli-amp is desirable for maintaining constant current through the cell bridge.

The conductivity cell itself was fairly accurate and stable, but it should be cleaned at intervals and checked frequently for possible drift of zero or potential bias of the setting made to read the initial calibration curve. Known samples are indispensable to the proper employment of the conductivity cell, and good mixing equipment and procedure should be employed for their preparation. The current and

voltage used in the cell bridge should be as high as possible for sensitivity but low enough to prevent fusing of the paired resistance wires.

III. 5. 2. Suggestions for Additional Coverage of the Cylinder Wake

Any new equipment designed for concentration studies in the wake should be checked against the results of Figure 15, which is the plot of points taken with the model in stable flow. Following check-out of the equipment, the profile data of this investigation should be repeated in the stable flow. The new data should include K_{max} points taken for various tunnel pressures in the turbulent Reynolds number regions. Extensive total and static pressure coverage of the same P_o and x/D points should be made to determine exchange coefficients. Extensive coverage of the necked region of the wake should be obtained to determine how initial conditions might affect the later similar flow. Comparison of the normalized profiles with error distributions and modified formulas from the empirical theory should be made. Variation of the helium flow is desirable to see what effects may result in the diffusion and pressure profiles. Another diffusing gas should be employed to determine the effects in this regard. A heavy gas for instance might be useful in determining the relative diffusion of mass and momentum as compared to the light gas of the present experiment. An extensive program of wake coverage as outlined will provide a good background for studies of all types in wakes and boundary layers, where binary gas components may be detected by the thermal conductivity method.

IV. CONCLUSIONS

The several important conclusions which may be derived from the present investigation are as follows:

(1) The thermal conductivity method is an important and useful one for diffusion studies in the hypersonic flow field, where one binary constituent is to be detected in another. The method is adequate in determining mass diffusion properties of a flow with a light gas injected as tracer or as coolant for the model.

(2) The problem of low densities in the samples taken from hypersonic flows can be controlled by suitable calibration. The procedure can be improved over that of the experimsnt with a more sensitive measurement of the sample pressures.

(3) Other improvement of the model, probe, and instrumentation will increase the accuracy of the method employed in this case to within one or two per cent error for concentrations on the order of one-half per cent.

(4) The method is adequate to determine turbulent processes of the flow and to detect transition, if the data is properly reduced and plotted to bring out the similarity properties.

(5) The wake of the hypersonic cylinder is formed from the boundary layer gas which is retained initially in shear layers at very low pressure behind the model, in trapezoidal shaped profiles of mass. The gases are compressed into a very narrow wake at a distance of about two diameters downstream of the model, after which the lateral diffusion rapidly approaches the similarity regime.

(6) The similar pattern is set up in either laminar or turbulent

flow at between 5 - 9 diameters behind the model. This result is in contrast to the much greater distances required in low speed flow.

(7) In the laminar case, the theoretically predicted scaling of the maximum concentration inversely as the square root of the supply pressure was satisfied in the ratio of the P_o = 10 and P_o = 35 psig readings. In the higher pressure cases (P_o = 60, 85), K_{max} did not scale with $1/P_o$ as an approximate consideration indicates. Either the dependence on the pressure is more involved in the turbulent case, or the fully turbulent flow was not yet reached at the highest Reynolds number of the experiment.

(8) Diffusion profiles were affected somewhat by a tunnel flow perturbation, but are still observed to be typically Gaussian, as theory predicts, a few diameters downstream of the narrowed portion of the wake.

REFERENCES

1. Goldstein, S.: Modern Developments in Fluid Dynamics, Vol. II - Wakes, Oxford University Press, 1938.

2. Pai, S. I.: Fluid Dynamics of Jets, D. Van Nostrand Company, Inc., Princeton, 1954.

3. Prandtl, L.: The Mechanics of Viscous Fluids, Durand: Aerodynamic Theory, Vol. III, pp. 34-207, Guggenheim Aeronautical Laboratory, 1934.

4. Townsend, A. A.: The Structure of Turbulent Shear Flow, Cambridge University Press, 1956.

5. Schubauer, G. B. and C. M. Tchen: Turbulent Flow, Turbulent Flows and Heat Transfer, Princeton Series in High Speed Aerodynamics and Jet Propulsion, Vol. V, Section B; (Editor: C. C. Lin), Princeton University Press, 1959.

6. Hinze, J. O.: Turbulence, Chapters II, V, and VI, McGraw-Hill Book Company, New York, 1959.

7. Lees, L.: Convective Heat Transfer with Mass Addition and Chemical Reactions, Combustion and Propulsion, Third AGARD Colloquium, Pergamon Press, 1958.

8. Mickley, H. S.; R. C. Ross; A. L. Squyers; W. E. Stewart: Heat, Mass and Momentum Transfer for Flow over a Flat Plate with Blowing or Suction, NACA TN 3208, July, 1954.

9. Low, G. M.: The Compressible Laminar Boundary Layer with Fluid Injection, NACA TN 3404, March, 1955.

10. Lees, L.: Laminar Heat Transfer over Blunt-Nosed Bodies at Hypersonic Flight Speeds, Jet Propulsion, Vol. 26, No. 4, pp. 259-269, April, 1956.

11. Tendeland, T. and Arthur F. Okuno: The Effect of Fluid Injection on the Compressible Turbulent Boundary Layer, NACA TR A56D05, June 19, 1956.

12. Rubesin, Norris W. and Constantine C. Pappas: An Analysis of the Turbulent Boundary Layer Characteristics on a Flat Plate with Distributed Light Gas Injection, NACA TN 4149, February, 1958.

13. McMahon, H. M.: An Experimental Study of the Effect of Mass Injection at the Stagnation Point of a Blunt Body, GALCIT Hypersonic Research Project, Memorandum No. 42, May 1, 1958.

14. Lees, L.: Recovery Dynamics - Heat Transfer at Hypersonic Speeds in a Planetary Atmosphere, Space Technology, Chapter 12, pp. 12-01 to 12-20, John Wiley and Sons, New York, 1959.

15. Lees, L.: Ablation in Hypersonic Flows, paper presented at the seventh Anglo-American Conference sponsored jointly by the R. Ae. S. and the I. A. S., New York, N. Y., October 5-7, 1959.

16. Rush, D. and W. Forstall, Jr.: Apparatus for the Determination of the Concentration of Helium in Air by the Thermal Conductivity Method, M. I. T. Internal Report No. 4 for Project Meteor, M. I. T. Gas Turbine Laboratory, January, 1947.

17. Forstall, W., Jr. and Ascher H. Shapiro: Momentum and Mass Transfer in Coaxial Gas Jets, Journal of Applied Mechanics, Vol. 17, No. 4, pp. 399-408, December, 1950.

18. Daynes, H. A.: Gas Analysis by Measurement of Thermal Conductivity, Cambridge University Press, 1933.

19. Eimer, M. and H. T. Nagamatsu: Direct Measurement of Laminar Skin Friction at Hypersonic Speeds, GALCIT Hypersonic Research Project, Memorandum No. 16, July 1, 1953.

20. Baloga, P. E. and H. T. Nagamatsu: Instrumentation of GALCIT Hypersonic Wind Tunnels, GALCIT Hypersonic Research Project, Memorandum No. 29, July 31, 1955.

21. Ames Research Staff: Equations, Tables, and Charts for Compressible Flow, NACA TR 1135, Ames Aeronautical Research Laboratory, 1953.

22. Liepmann, H. W. and A. Roshko: Elements of Gas Dynamics, Chapters VI and XIV, John Wiley and Sons, Inc., New York, 1957.

23. Bomelburg, H. J.: Heat Loss from Very Thin Heated Wires in Rarefied Gases, The Physics of Fluids, Vol. 2, No. 6, pp. 717-718, November-December, 1959, American Institute of Physics.

TABLE I

SUMMARY OF GAS PROPERTIES

(1)	(2)	(3)	(4)	(5)
Gas	Molecular Weight	Ratio of Conductivity to Air at 0°C	Temperature Coefficient of Conduction 0 - 100°C, per °C	Per Cent in Dry Air at Sea Level By Mass
Air	28.97	1.00	.00265	
Carbon Dioxide	44.01	.605	.00527	.05
Helium	4.003	5.97	.00256	trace
Hydrogen	2.016	7.15	.00265	trace
Nitrogen	28.02	.996	.00264	75.80
Oxygen	32.00	1.013	.00303	23.22
Argon	39.99	.685	.00311	.94
Water Vapor	18.02	.725 (46°C)	.00540	0 - 6.0

Column References:

(2) Handbook of Chemistry and Physics, 1st edition

(3), (4) Daynes, Gas Analysis by Measurement of Thermal Conductivity, Table 1, Cambridge University Press, 1933

(5) Aeronautical Handbook, Pratt and Whitney Aircraft Company, 1957

TABLE II

CONCENTRATION TEST DATA SHEET

Run No. _____ Date _____

Type of Run _____

(1) Tunnel Conditions

M = 5.8; T_o = 275°F

P_o = _____ psig

(2) Model Installation Check

Vac. pump vs. chamber _____

Vac. pump vs. model _____

Difference, (cm Hg) _____

(3) Room Conditions

Bar. Press. P_{b_s} cm Hg	Temp. °C	Time

Ref. Bar Press, P_{br} = _____ cm Hg.

(4) Instrument Check

zero bridge tare _____ mv

Sample correction ratio, for bridge bias _____/_____

(5) Helium Flow Data

He on at _____:_____ psig

He off at _____:_____ psig

Flowrator setting _____

Metering pressure _____ cm Hg

Metering temperature _____ °C

Tunnel Conc., mv	Time

(6)

x/d	Time	Probe y, in.	Sample Δp, cm Hg	emf mv

TABLE III

CONCENTRATION DATA REDUCTION SHEET

Test No. _____ Date _____ Test Type _____

Flow: M = 5.8; T_o = 275°F; $\dot{m}_{He}$ = .0031 lb/min; P_o = _____ psig

Tunnel Concentration, T. C. = _____ mv*; Sample Ratio, S. C. = _____

(1)	(2)	(3)	(4)	(5)	(6)	(7)	(8)	(9)	(10)	(11)	(12)
x/D	y, in.	y - CL in.	y/D	emf, mv	(5)-T. C. mv	(6)(S. C.) mv	p, cm Hg	$\frac{p^{**}}{p_{bs}}$	emf (Fig. 6)	(7)+(10) = emf	K (Fig. 5)

* correct for variable T. C. when applicable

** barometer pressure, p_{bs}, from time plot, when $p/p_{bs} > .99$

TABLE IV

ERROR ESTIMATE

(1) Item	(2) Cause	(3) Amount	(4) Range of Error	(5) Possible Remedy
1. helium flow setting	low sensitivity of flowmeter	$\pm$ 3.5% of emf (mv)	all readings	more sensitive meter
2. zero shift	unstable T.C. cell, ammeter, and potentiometer	$\pm$ .05 mv	all readings	stable sensitive instruments; monitor current closely; keep cell clean
3. pressure calibration error	low sensitivity of pressure scale	$\pm$ 8% to 0% of mv	K = 5% at $\Delta p/p_{bs}$ = 1.0 to $\Delta p/p_{bs} < .5$	use micromanometer on pump scale; measure Δp to .1 mm Hg

4. Miscellaneous small effects having less than 1% aggregate error for average concentration readings of the tests:

   a. temperature difference
   b. probe setting
   c. model differences
   d. oil in flow
   e. vibration
   f. helium impurity (from lines)
   g. tunnel conditions off by $\pm$ .2 psi and 2°F

5. Intermittent errors (large ones can usually be detected):

   a. water vapor in flow caused by excess make-up air with insufficient drying
   b. model installation or helium line leakage after metering
   c. large contamination in conductivity cell
   d. bad leaks in sampling system

Total possible error for a sample of 1% helium concentration at pressure ratios $\Delta p/p_{bs} < .9$ is approximately 6 % .

TABLE V

TEST REYNOLDS NUMBERS

$T_o = 275^{\circ}F$ = constant		
P_o, psig	$Re/in \times 10^{-4}$ *	$Re_D \times 10^4$ *
10	5.52	1.66
35	11.18	3.35
60	16.82	5.05
85	22.48	6.75

* Based on atmospheric pressure of 14.4 psi for the laboratory elevation, and cylinder diameter, D = 0.30 inch

TABLE VI

LIST OF PRESSURE DATA

	Total Pressure								
(1)	(2)	(3)	(4)	(5)	(6)	(7)	(8)	(9)	(10)
Run	Fig. No.	Date	P_o	x/D	Probe Position, z Direction	Model Type	He Flow lb/min	Corresponding Concentration Runs	Flow Conditions
1	16, 19	12/31/59	85	5	center	porous	0	1-5	Runs 1-5:
2	19	"	85	5	"	"	.003	1-5	forward
3	18	"	10	5	"	"	.003	1-5	position -
4	19	1/4/60	85	5	1 in. off	"	.0031	off center	somewhat
5	19	"	85	5	"	"	0	corresponds	erratic
6	18	"	10	5	"	"	0	to runs with	Runs 8, 9:
7	18	"	10	5	"	"	.0031	model in rear	first flow
8	16, 19	1/19/60	85	5	center	brass	0	position,	shift, fwd.
9	19	"	85	5	"	porous	0	runs 10-13	position
(flow shifted again for concentration runs 6-9, wherein no P_o traverses were made)									
10	18	3/22/60	10	5	center	porous	0	10-15	Runs 10-13:
11	17	3/23/60	60	5	"	"	0	10-15	model
12	17	"	35	5	"	"	0	10-15	moved to
13	16	3/25/60	85	5	"	"	0	10-15	rear
14	17	"	60	5	"	"	0	10-15	model forward

This table is continued on the following page.

TABLE VI -- CONTINUED

Total Pressure									
(1) Run	(2) Fig. No.	(3) Date	(4) P_o	(5) x/D	(6) Probe Position, z Direction	(7) Model Type	(8) He Flow lb/min	(9) Corresponding Concentration Runs	(10) Flow Conditions
traverses made by McCarthy with brass model									
15	16	6/8/59	85	5	center	brass	0	1-5	Runs 15-22:
16	17	6/15/59	60	5	"	"	0	1-5	flow
17	17	"	35	5	"	"	0	1-5	conditions
18	18	6/16/59	10	5	"	"	0	1-5	close to
19	21	8/17/59	10	9	"	"	0	1-5	Runs 1-7
20	20	8/25/59	85	15	"	"	0	1-5	above
21	21	"	10	15	"	"	0	1-5	
22	20	10/21/59	85	20	"	"	0	1-5	

This table is continued on the following page.

TABLE VI -- CONTINUED

Measured Static Pressures at Wake Centerline (P_o/p)				
P_o	x/D			
	5.0	9.0	15.0	20.0
0.0	---	500	1120	----
10.0	730	561	1057	1173
15.0	---	587	----	----
20.0	---	610	----	----
25.0	---	629	----	----
35.0	780	659	1006	1401
60.0	800	695	984	1327
75.0	---	707	----	----
85.0	810	---	990	1124

p = static pressure (absolute)

P_o = tunnel reservoir pressure (psig)

TABLE VII

SUMMARY OF CONCENTRATION DATA

All Runs: $M = 5.8$; $T_o = 275^{\circ}F$; $\dot{m}_{He} = 0.00305 \pm .0001$ lb/min

(1) Run No.	(2) Fig. No.	(3) Date	(4) P_o, psig	(5) Type of Run	(6) x/D	(7) Remarks
1	10	11/23/59	85	Profile	3	
2	10	11/30/59	85	Profiles	9, 5	
3	10, 13	12/3/59	85	Profile	15	$\dot{m}_{He}$*= .00279 lb/min
4	11, 15	12/22/59	10	Profile	3	
5	11, 15	12/23/59	10	Profiles	9	$\dot{m}_{He}$*= .00307 lb/min
					15	$\dot{m}_{He}$*= .00281 lb/min
					24	
6	14	1/29/60	85	K_{max} pts	3, 5 6.5 8, 9	Flow shifted slightly since runs 1-5
7	14	2/2/60	85	K_{max} pts	9, 12, 15	
8	14	2/4/60	85	K_{max} pt.	28	
	12			$\frac{1}{2}$ Profile	20, 36	$\dot{m}_{He}$*=.00300 lb/min for x/D = 20
9	14	2/29/60	85	K_{max} pts	9, 5, 6, 5, 3 4, 2, 12, 20	
	12, 13			Profile	15	
10	14, 15	3/18/60	85	K_{max} pt	4	Runs 10-15: Basic flow shifted again since runs 6-9. Model position now 2.6" aft of position for runs 1-9.
11	15	3/21/60	10	K_{max} pts	3, 7	
12	15	3/22/60	10 35	K_{max} pts	5, 20, 27, 1 5, 15, 20	
13	15	3/23/60	35 60	K_{max} pts	5, 27, 9, 2 2, 5, 9, 20	

* $\dot{m}_{He}$ values refer to continuity check. See Section III. 4.

This table is continued on the following page.

TABLE VII-- CONTINUED

(1) Run No.	(2) Fig. No.	(3) Date	(4) P_o, psig	(5) Type of Run	(6) x/D	(7) Remarks
14	15	3/24/60	60	K_{max} pts	5, 3, 7, 15, 27	
				Profile	1	
	14, 15		85	K_{max} pts	9, 5, 3, 2, 1.5, 18, 27	
15	14, 15	3/25/60	35	K_{max} pts	3, 1	
			85		1, 7	

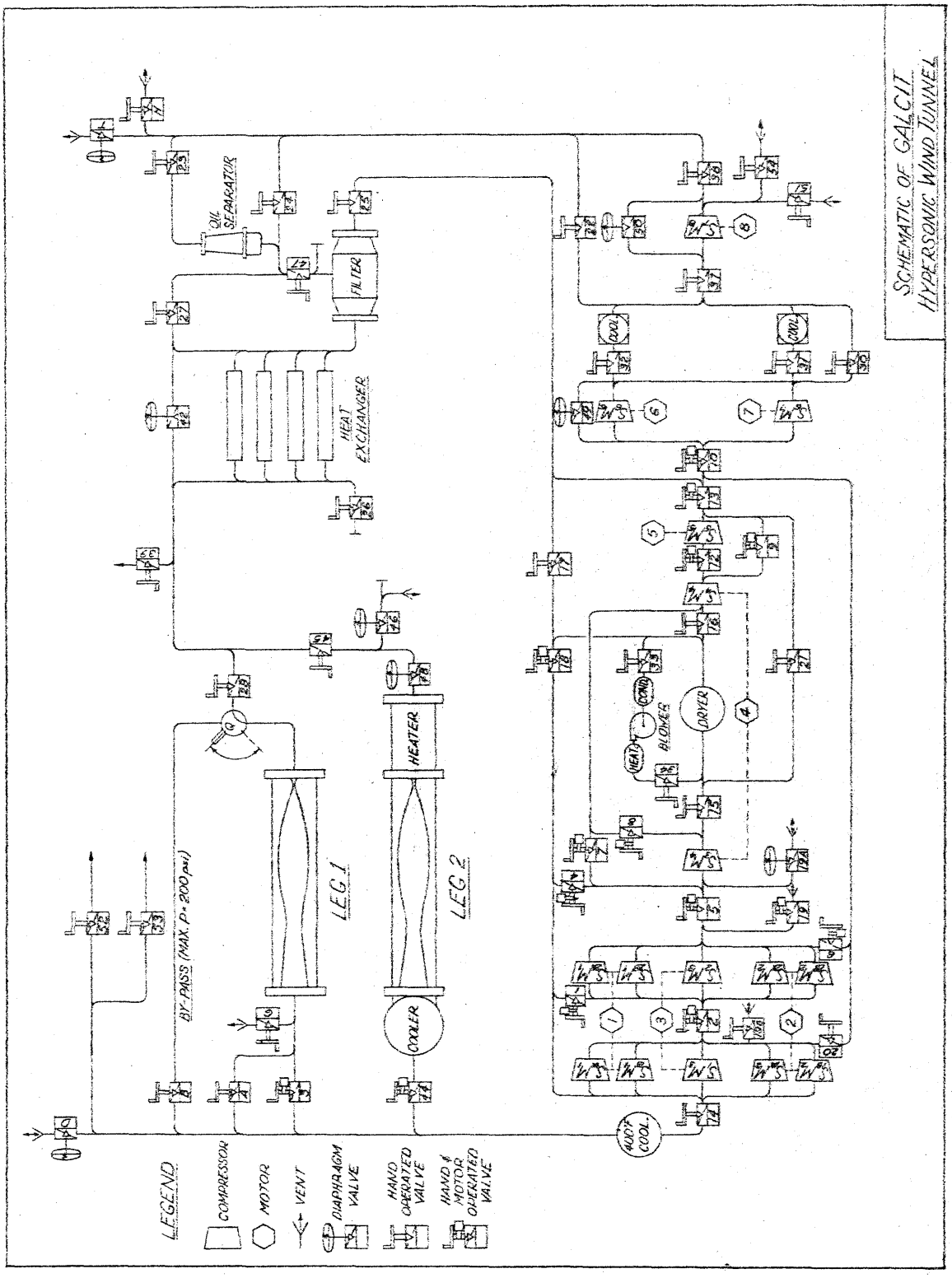
SCHEMATIC OF GALCIT
HYPERSONIC WIND TUNNEL
OIL SEPARATOR
FILTER
HEAT EXCHANGER
HEATER
COOLER
LEG 1
LEG 2
BY-PASS (MAX. P = 200 psi)
DRYER
BLOWER
HEAT
COOL.
LEGEND
COMPRESSOR
MOTOR
VENT
DIAPHRAGM VALVE
HAND OPERATED VALVE
HAND & MOTOR OPERATED VALVE

FIG. 1

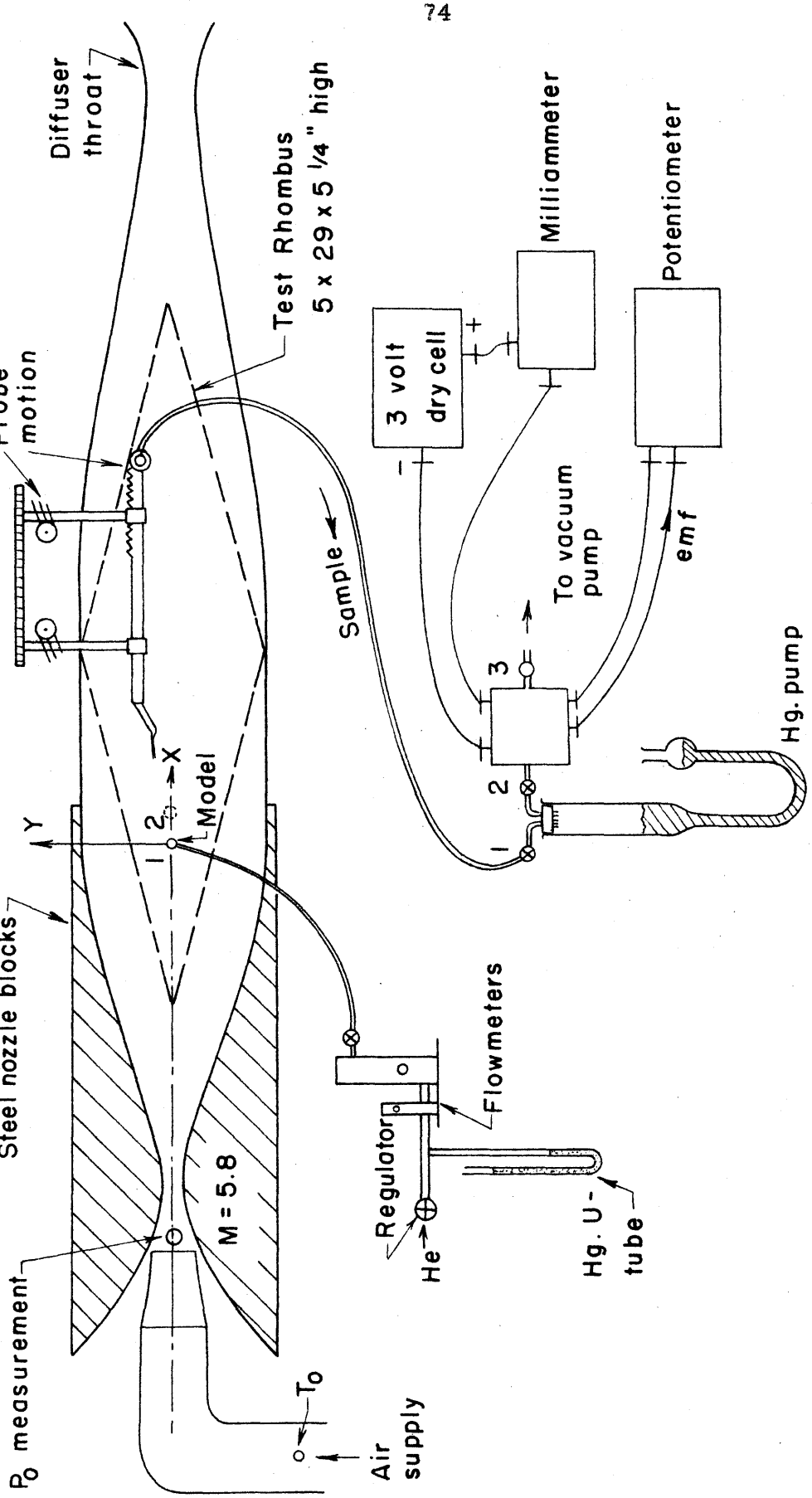

FIG. 2 DIAGRAM OF TEST SECTION AND EQUIPMENT, LEFT SIDE LEG I - FACING STREAM

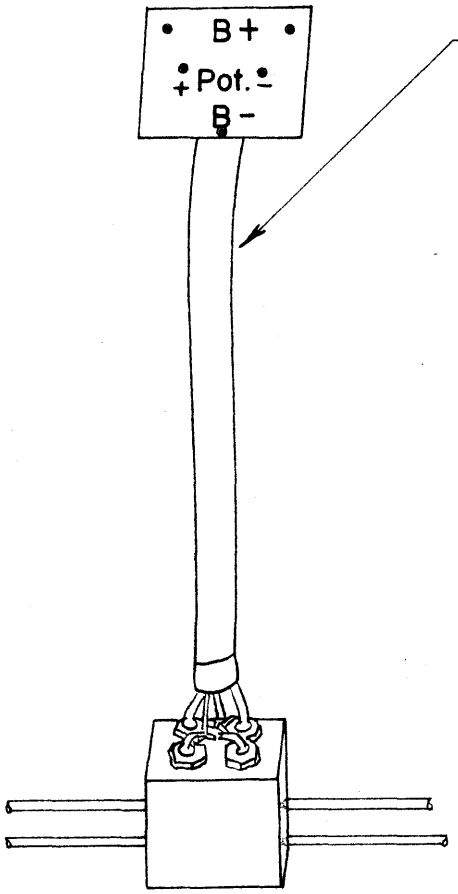

5 feed-through connectors wired in full Wheatstone bridge. Fiber-glass insulating sleeve, 12" leads.

For chromatography to 300° C.

Gow-Mac Instrument Co.
Madison, N.J.
Model 9285 with wiring
mod. 9193 (Te-11)
Tungsten filaments
Dimensions of cell:
2 x 2 x 2 5/8"

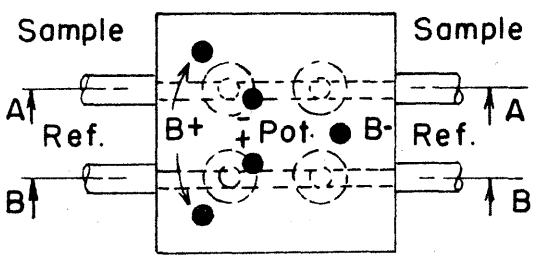

Top View

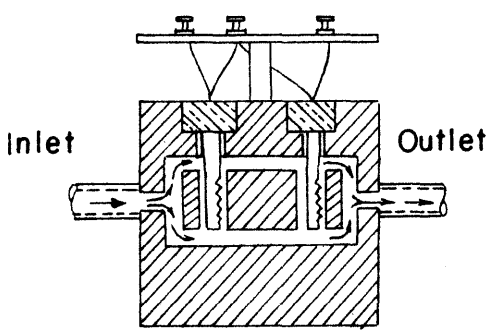

Sect. A-A
Sect. B-B

FIG. 3 THERMAL CONDUCTIVITY CELL

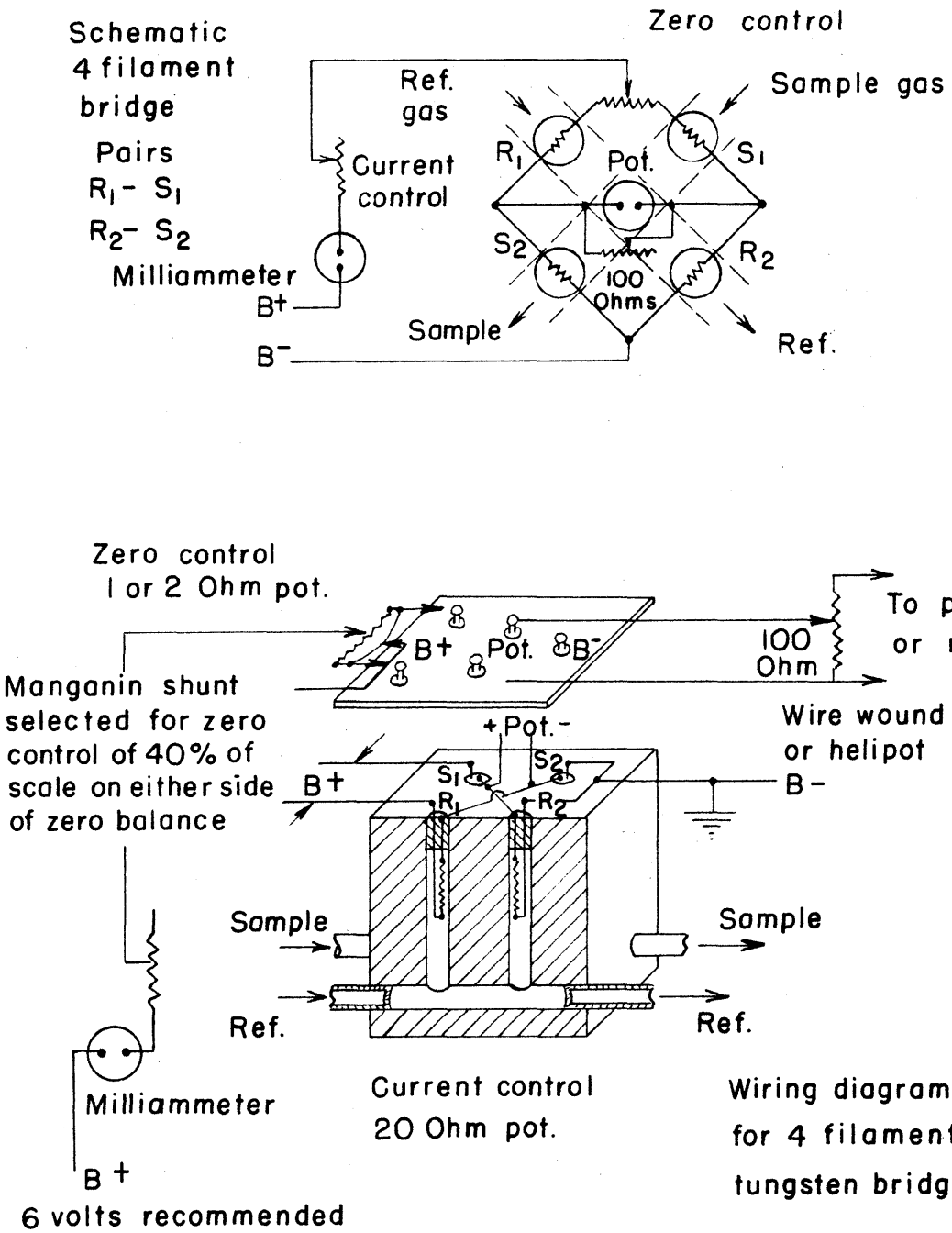

FIG. 4 DIAGRAM OF WIRING FOR THERMAL CONDUCTIVITY BRIDGE

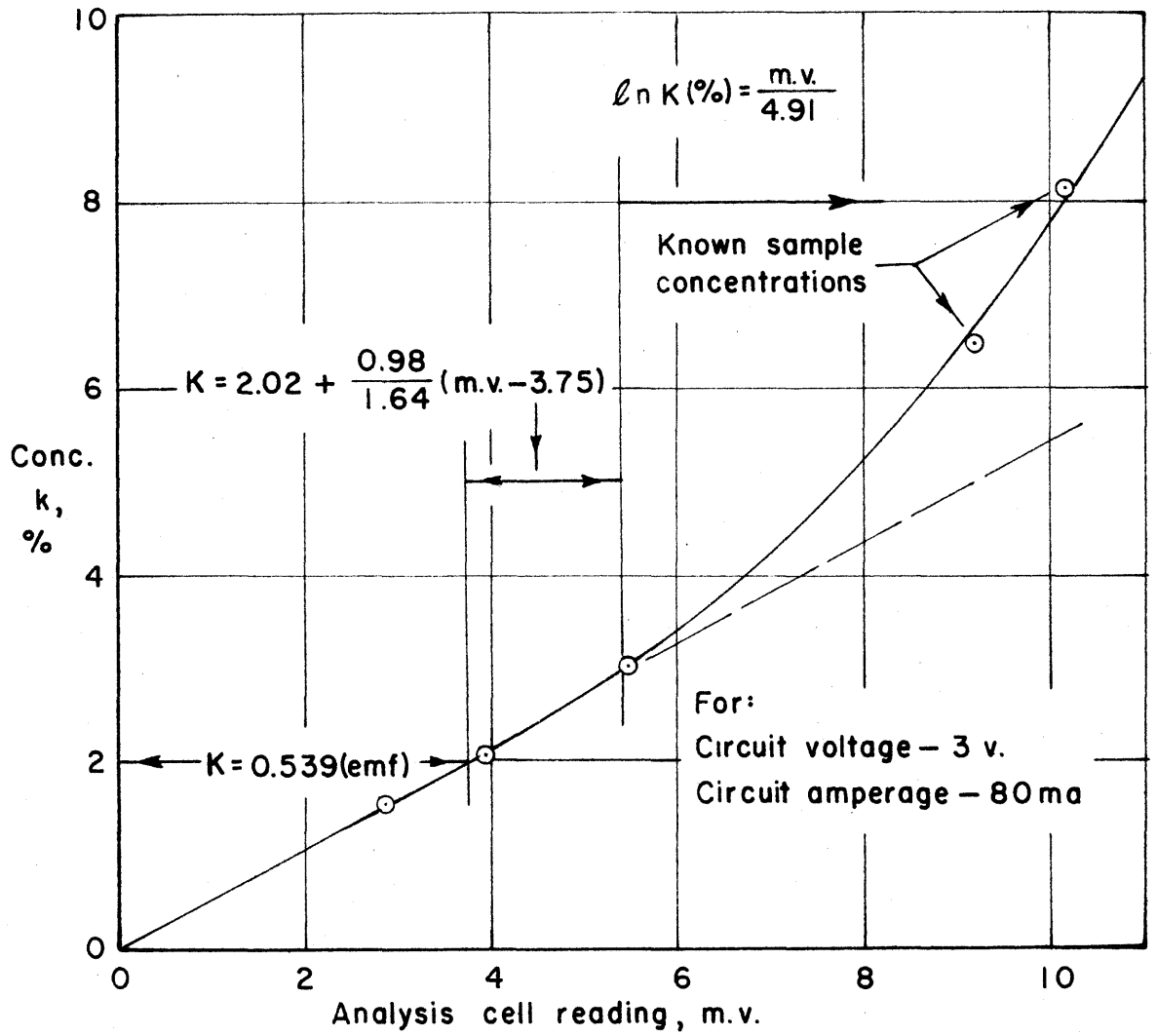

FIG. 5 MASS CONCENTRATION OF He IN N_2 VS. BRIDGE DEFLECTIONS

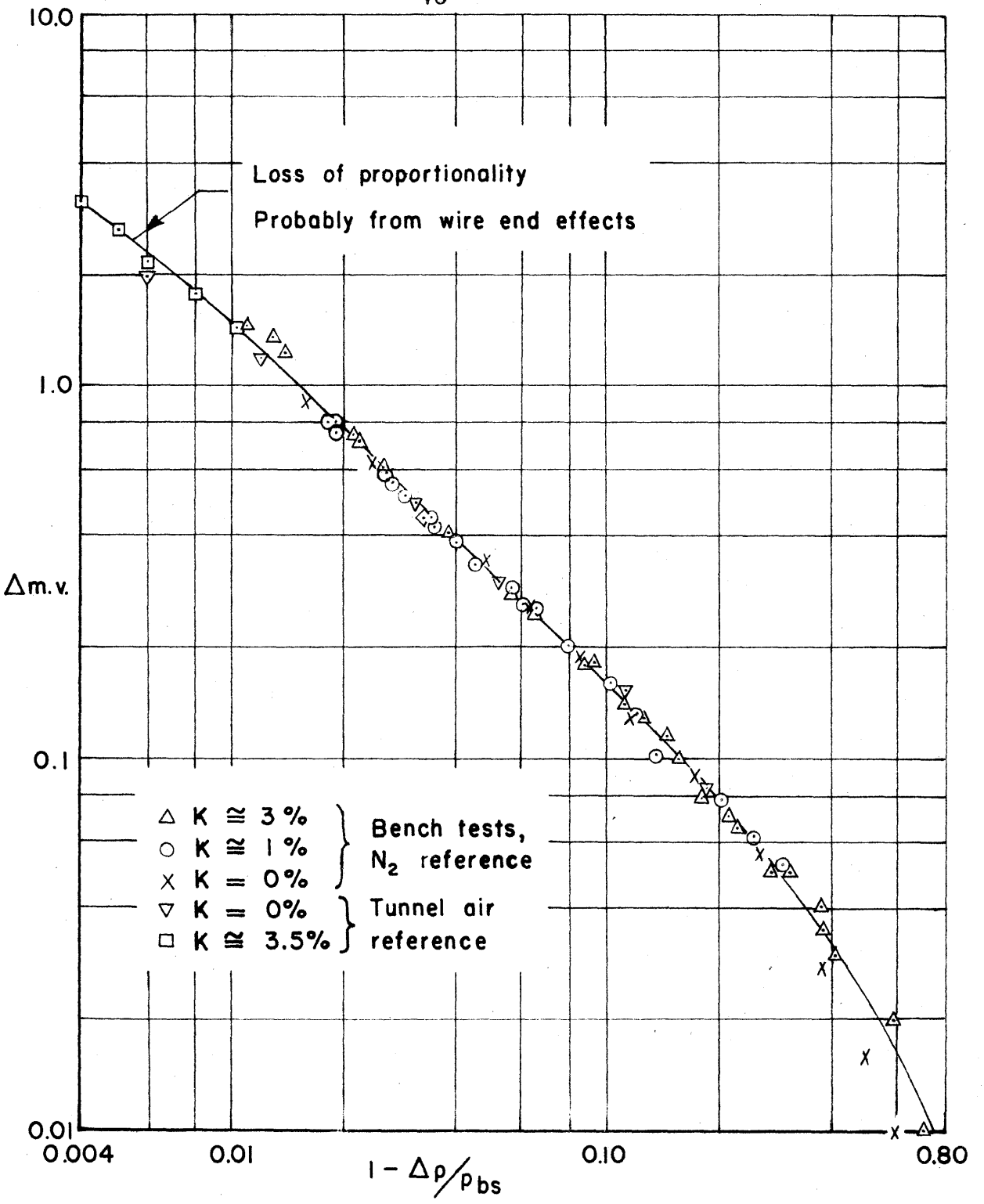

FIG. 6 CALIBRATION OF CONDUCTIVITY CELL FOR PRESSURE DIFFERENCE BETWEEN SAMPLE AND REFERENCE CHAMBERS

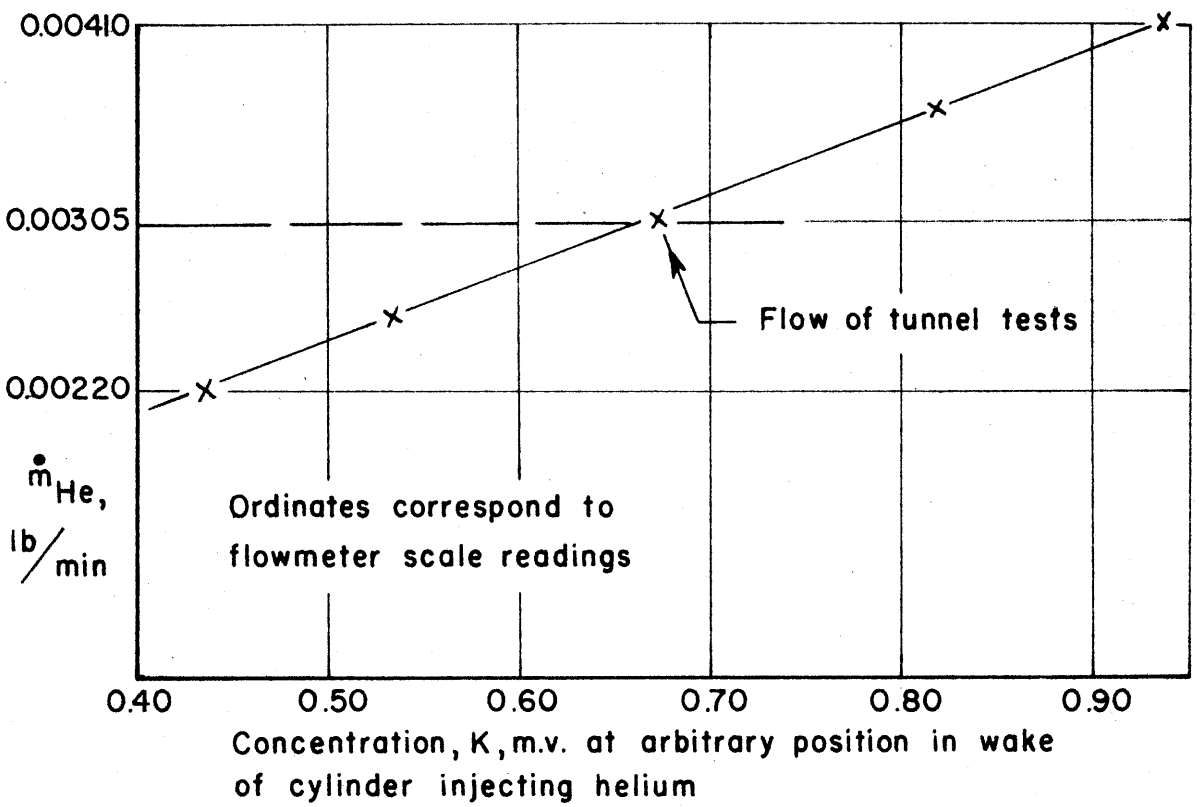

FIG. 7 LINEARITY OF CONCENTRATION WITH A SMALL CHANGE IN FLOW OF HELIUM

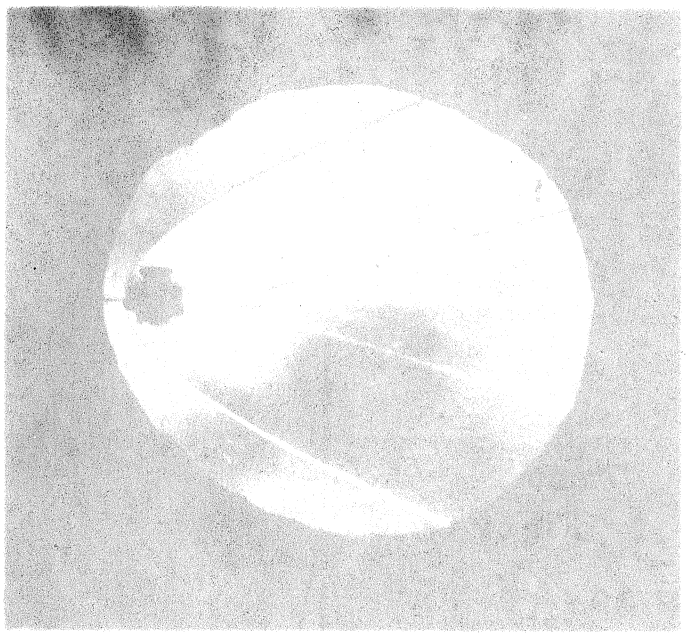

FIG. 8 -- SCHLIEREN PHOTOGRAPH OF POROUS CIRCULAR CYLINDER, M = 5.8 at P_o = 60 psig, T_o = 275°F (extraneous pattern caused by oil in flow; model shape affected by chips in glass)

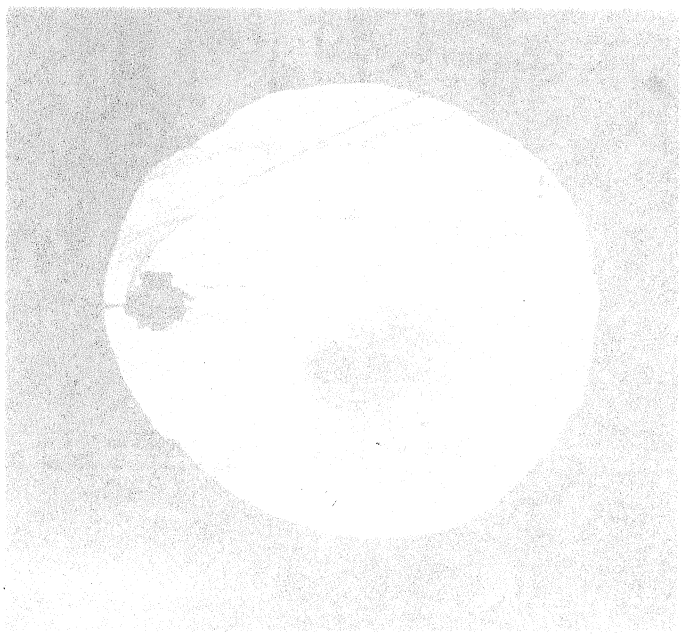

FIG. 9 -- SCHLIEREN PHOTOGRAPH OF POROUS CIRCULAR CYLINDER, M = 5.8 at P_o = 35 psig, T_o = 275°F

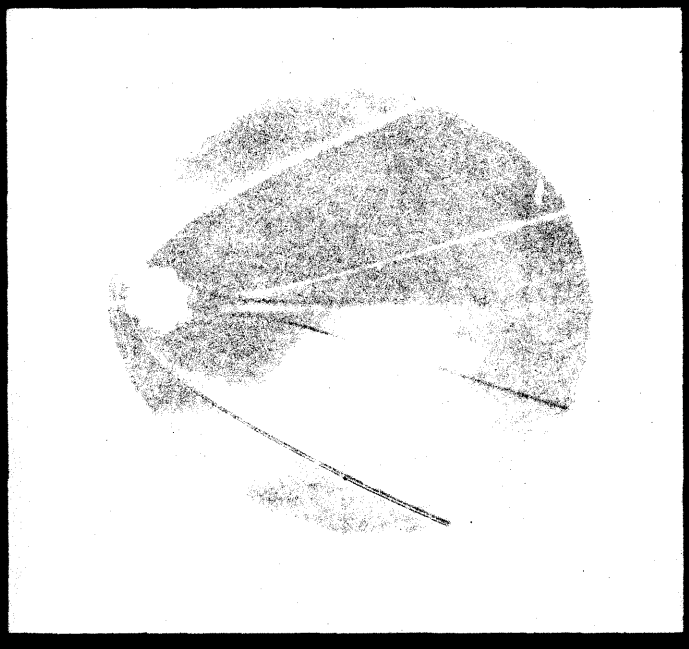

FIG. 8 -- SCHLIEREN PHOTOGRAPH OF POROUS CIRCULAR CYLINDER, M = 5.8 at P_o = 60 psig, T_o = 275°F (extraneous pattern caused by oil in flow; model shape affected by chips in glass)

FIG. 9 -- SCHLIEREN PHOTOGRAPH OF POROUS CIRCULAR CYLINDER, M = 5.8 at P_o = 35 psig, T_o = 275°F

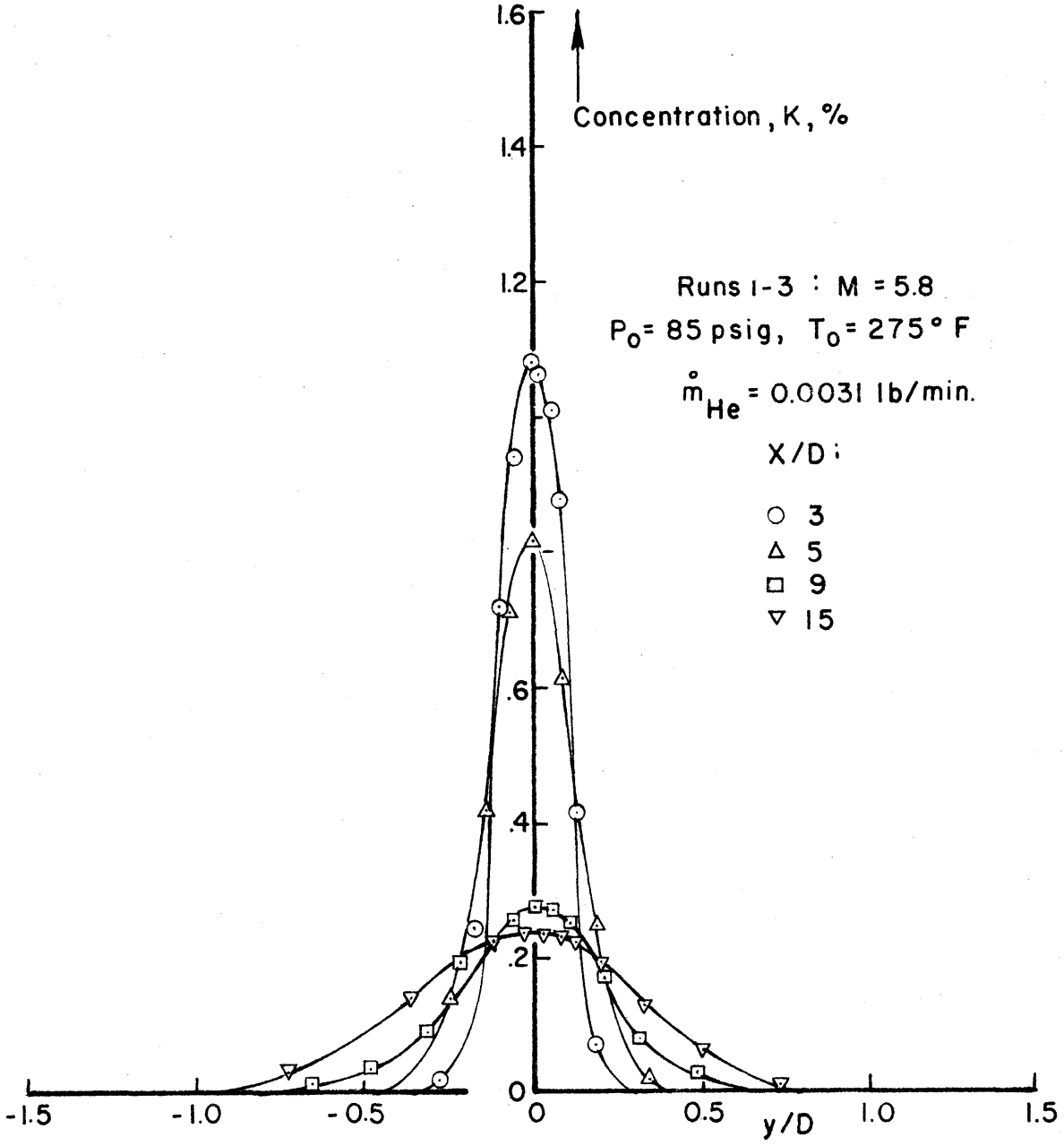

FIG. 10 HELIUM CONCENTRATION PROFILES IN THE WAKE OF A POROUS CIRCULAR CYLINDER

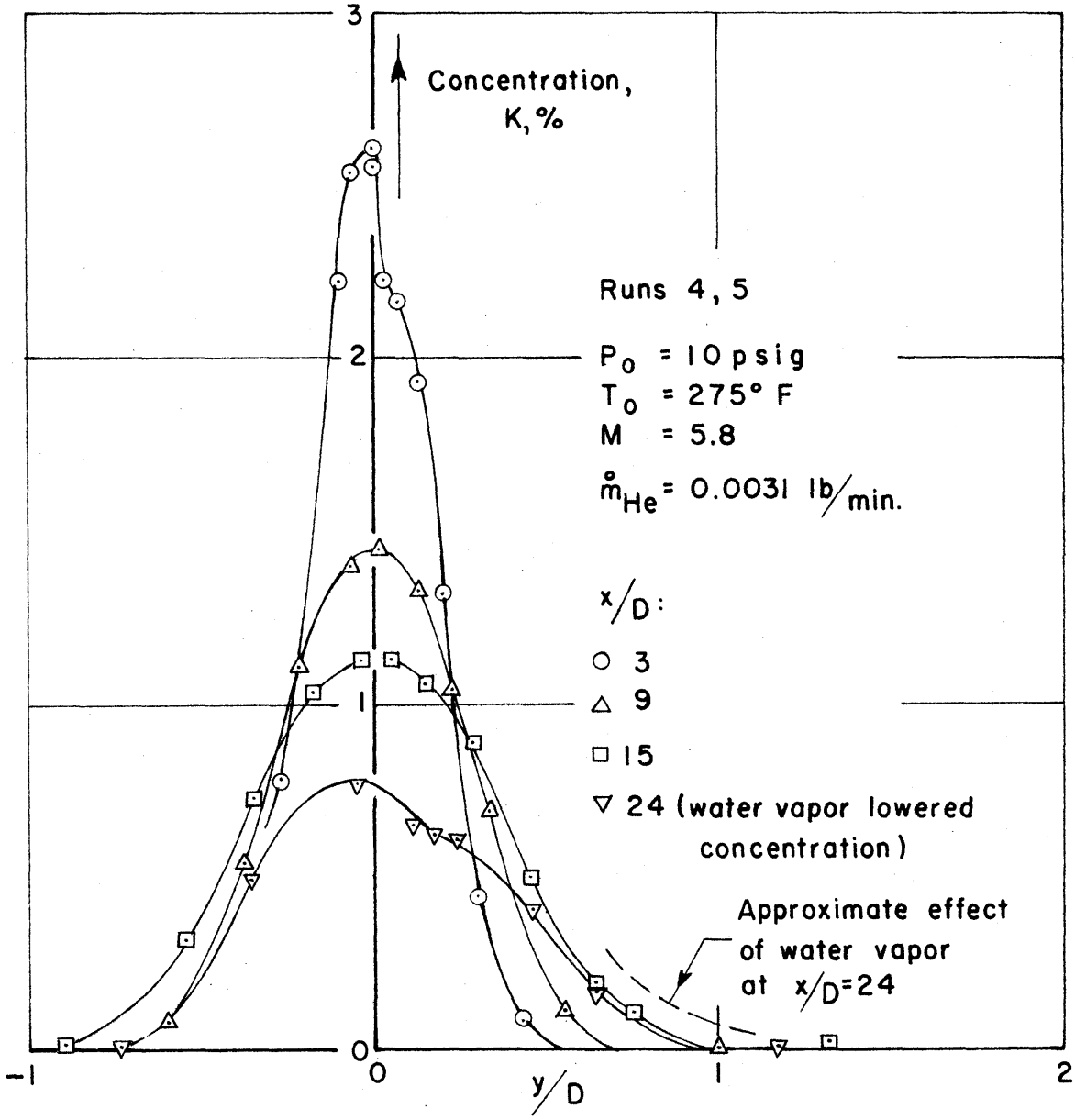

FIG. 11 HELIUM CONCENTRATION PROFILES IN THE WAKE OF A POROUS CIRCULAR CYLINDER

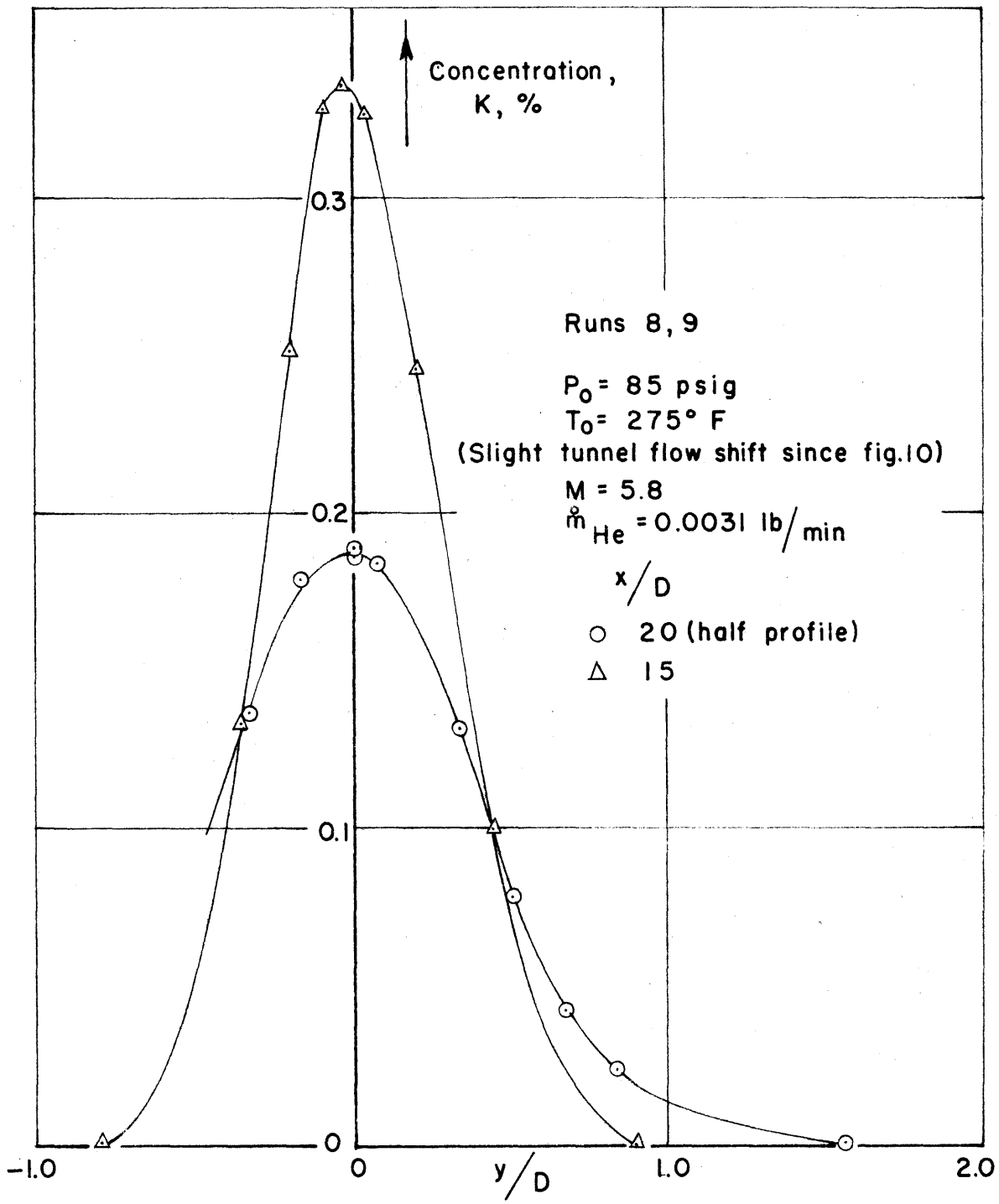

FIG. 12 HELIUM CONCENTRATION PROFILES IN THE WAKE OF A POROUS CIRCULAR CYLINDER

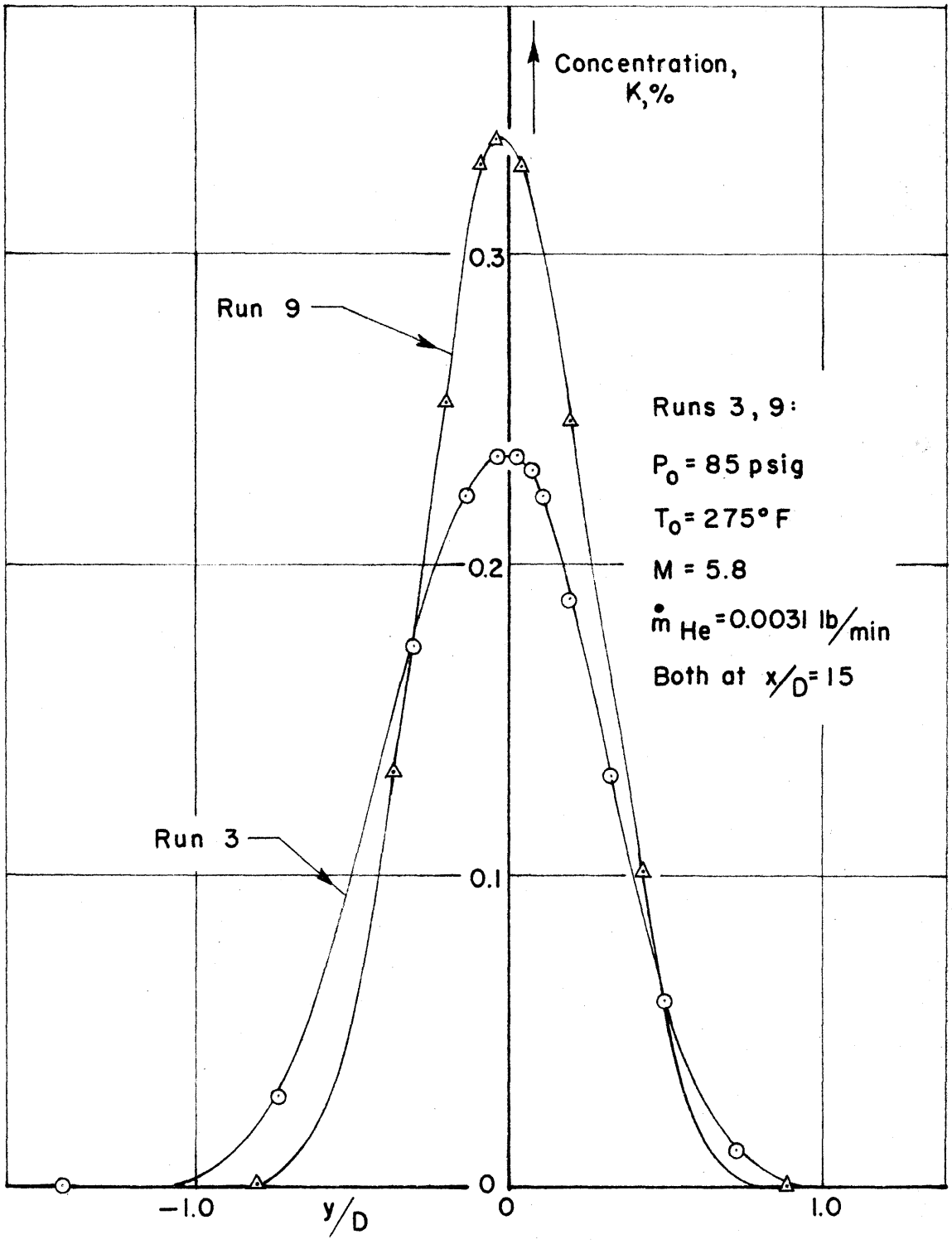

FIG. 13 COMPARISON OF PROFILES BEFORE AND AFTER SLIGHT TUNNEL FLOW SHIFT

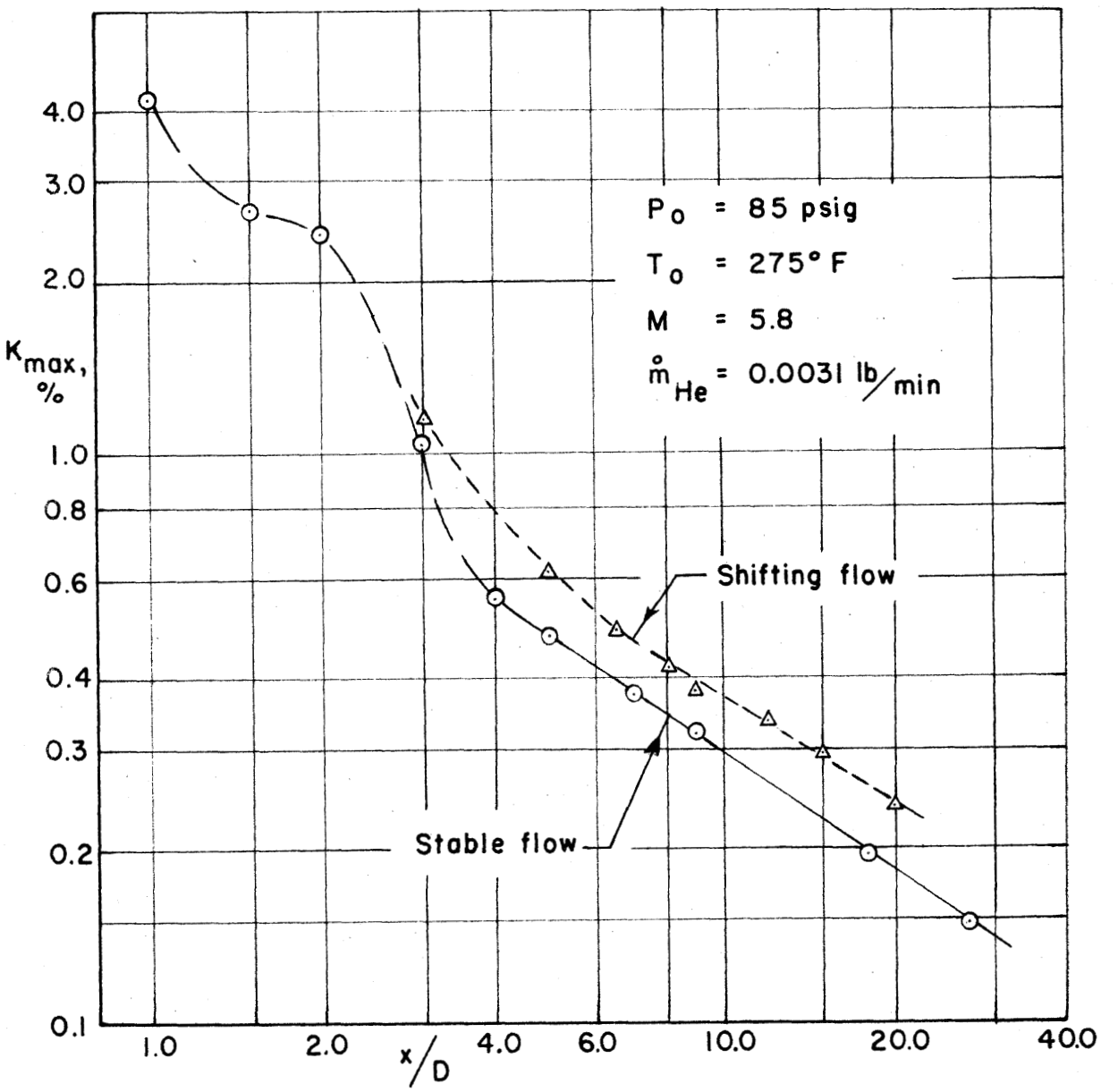

FIG. 14 PLOT OF K_{max} VERSUS x/D BEFORE AND AFTER TUNNEL FLOW SHIFT

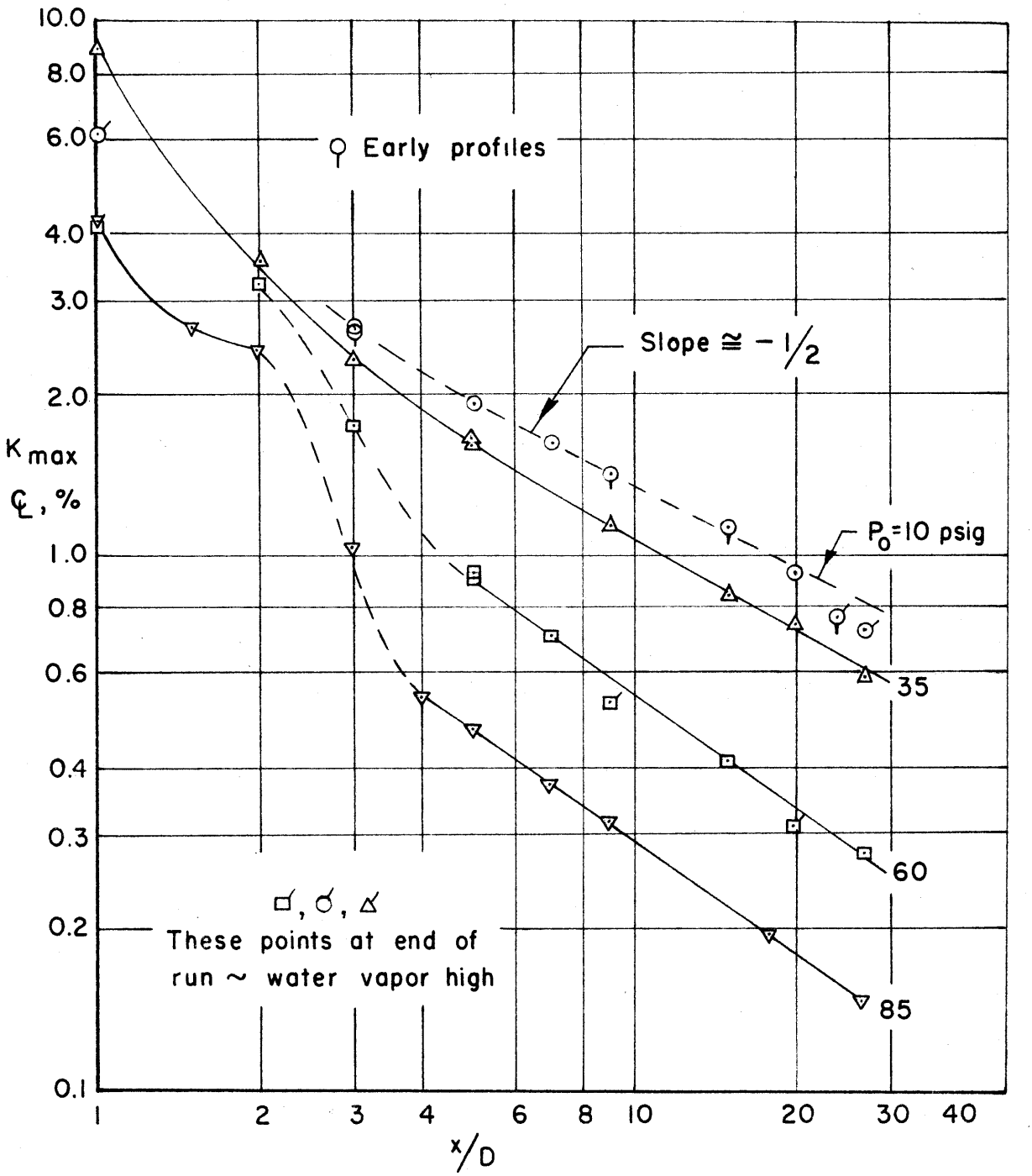

FIG. 15 PLOT OF MAXIMUM CONCENTRATION VERSUS AXIAL DISTANCE

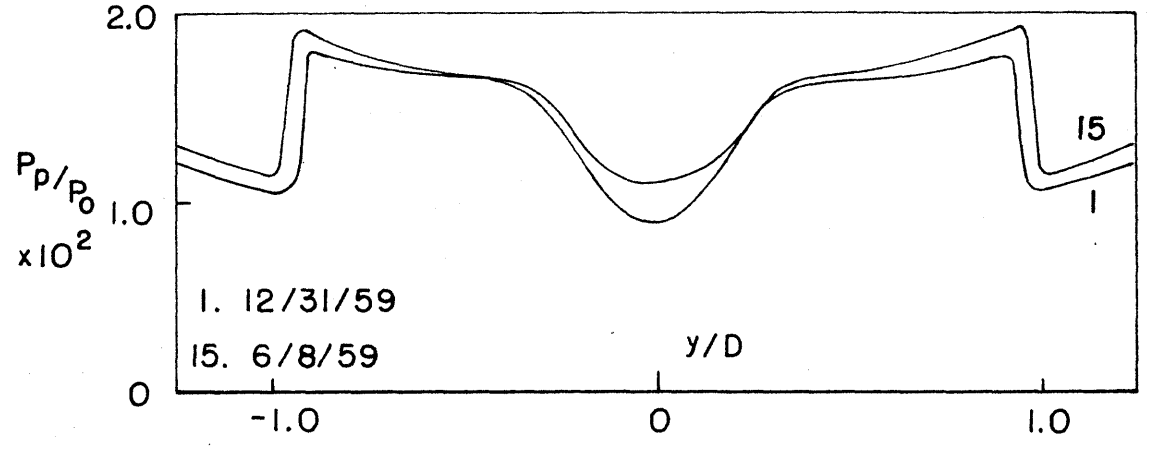

a. Comparison of flow for $P_o = 85$, $x/D = 5$, model fwd., probe centered

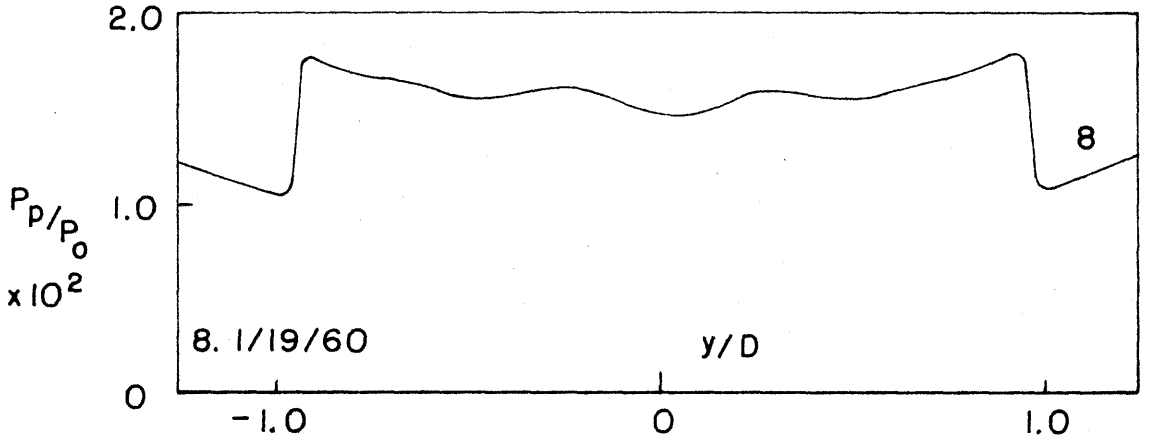

b. Same parameters as a , flow shift

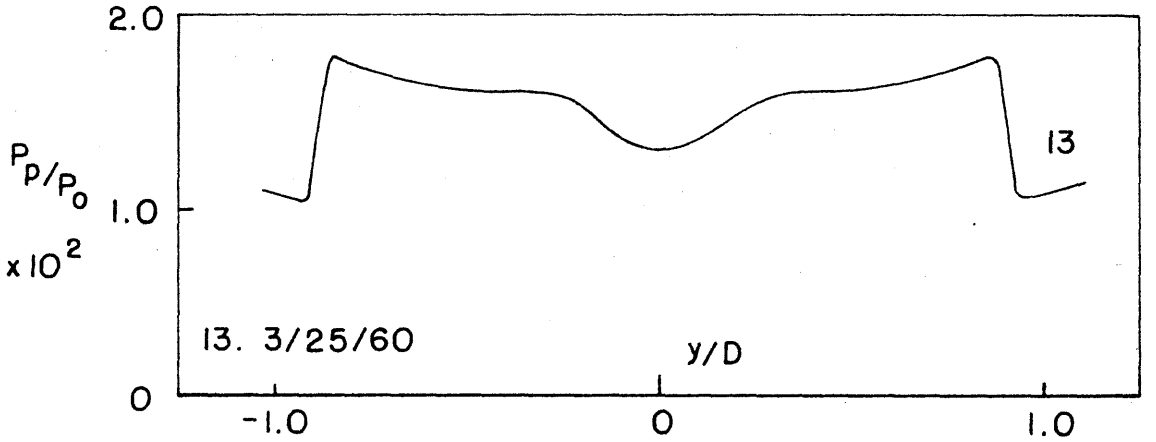

c. Model at rear position, stable

FIG. 16 FLOW SHIFTS WITH MODEL AT FWD. POSITION COMPARED WITH STABLE PLOT (C)

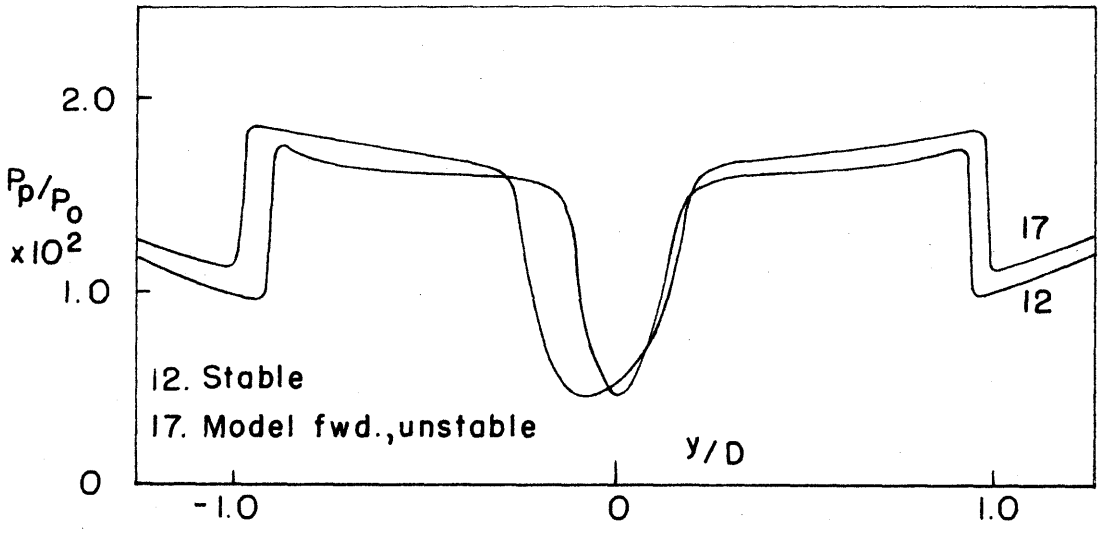

a. P_0 = 35, x/D = 5, model fwd., probe centered, $\dot{m}_{He} = 0$

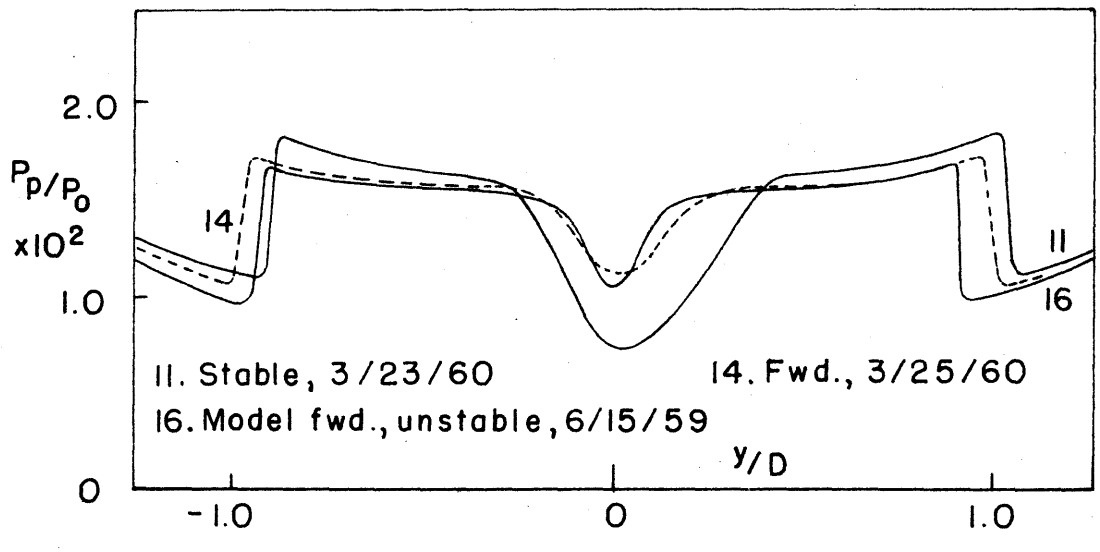

b. Same as a, except P_0 = 60

FIG.17 COMPARISON OF TOTAL PRESSURE TRAVERSES WITH MODEL IN STABLE AND SHIFTING FLOW

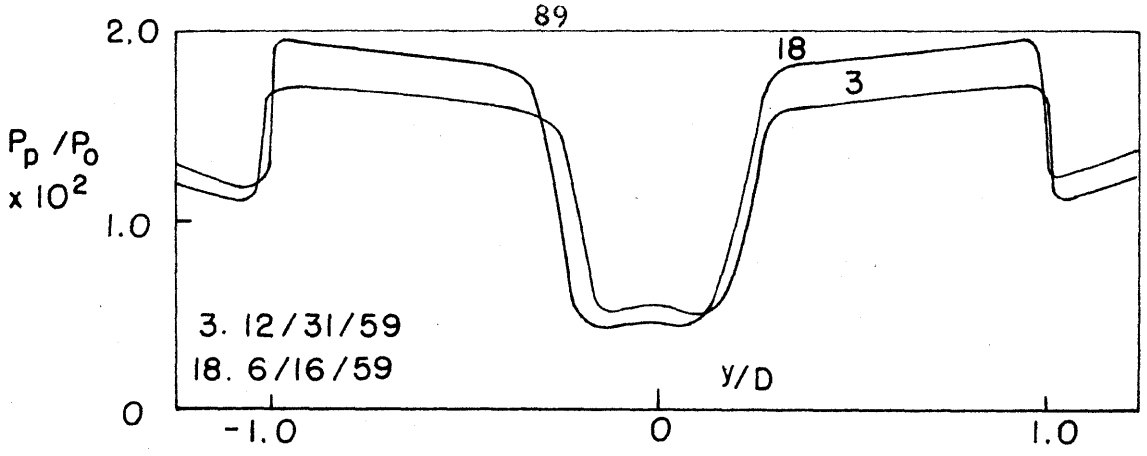

a. P_o = 10, x/D = 5, model fwd., probe centered

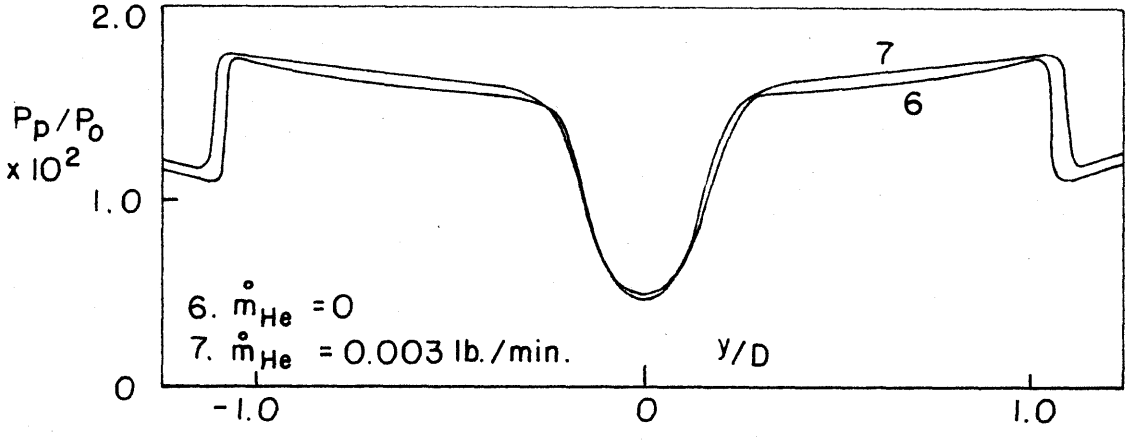

b. P_o = 10, x/D = 5, model fwd., probe at z = 1 in. off center

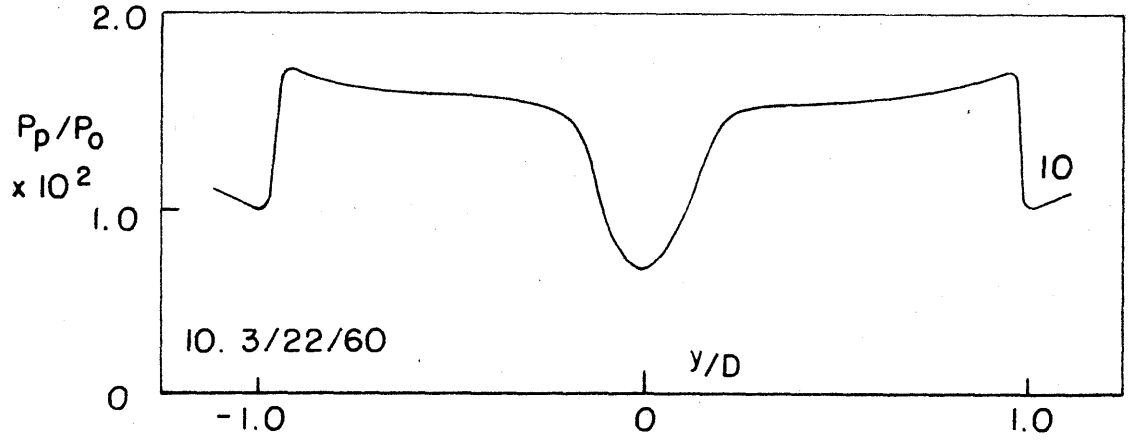

c. Model at stable rear position, P_o = 10, x/D = 5

FIG. 18 COMPARISON OF FLOWS FOR STABILITY AND MODEL POSITION

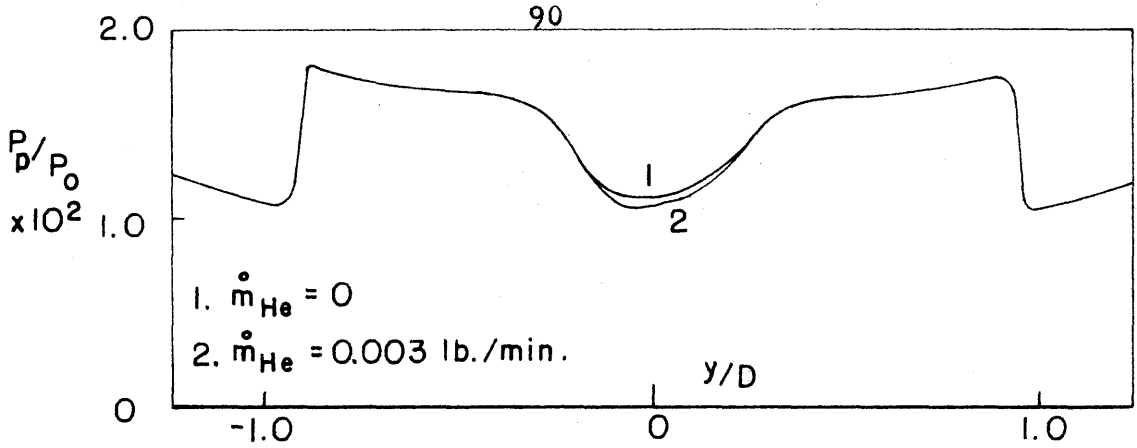

a. With and without Helium flow, model fwd., probe centered

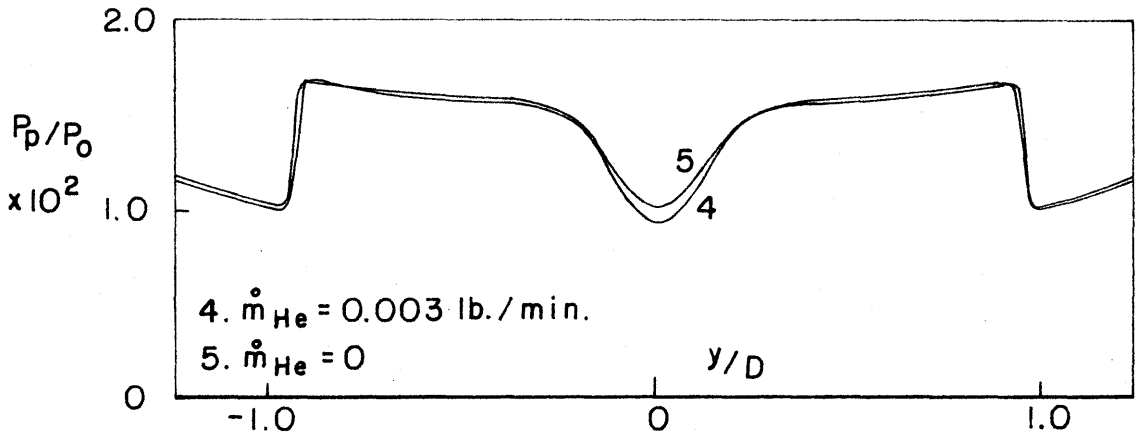

b. With and without Helium flow, model fwd., probe at z = 1.0 "

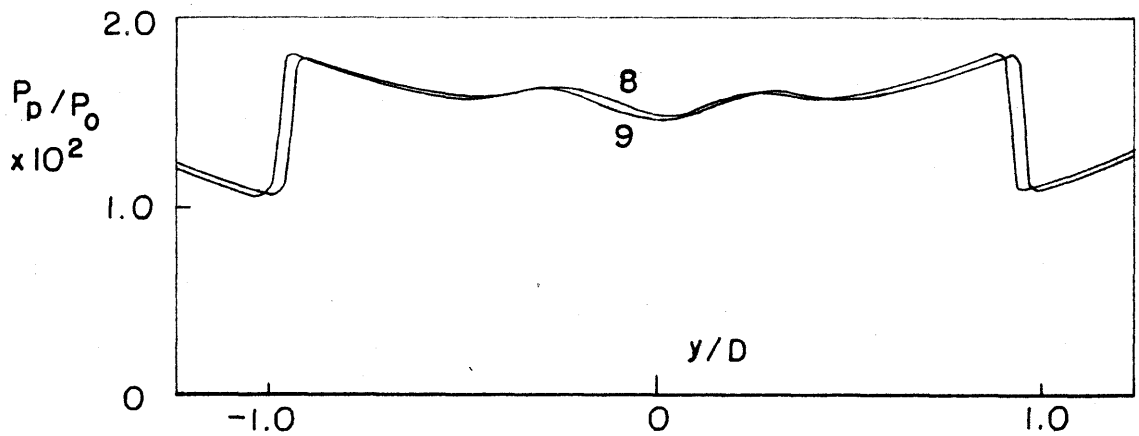

c. Duplicate trace for brass, porous models

FIG. 19 FLOW COMPARISONS AT $P_o = 85$ AND x/D = 5

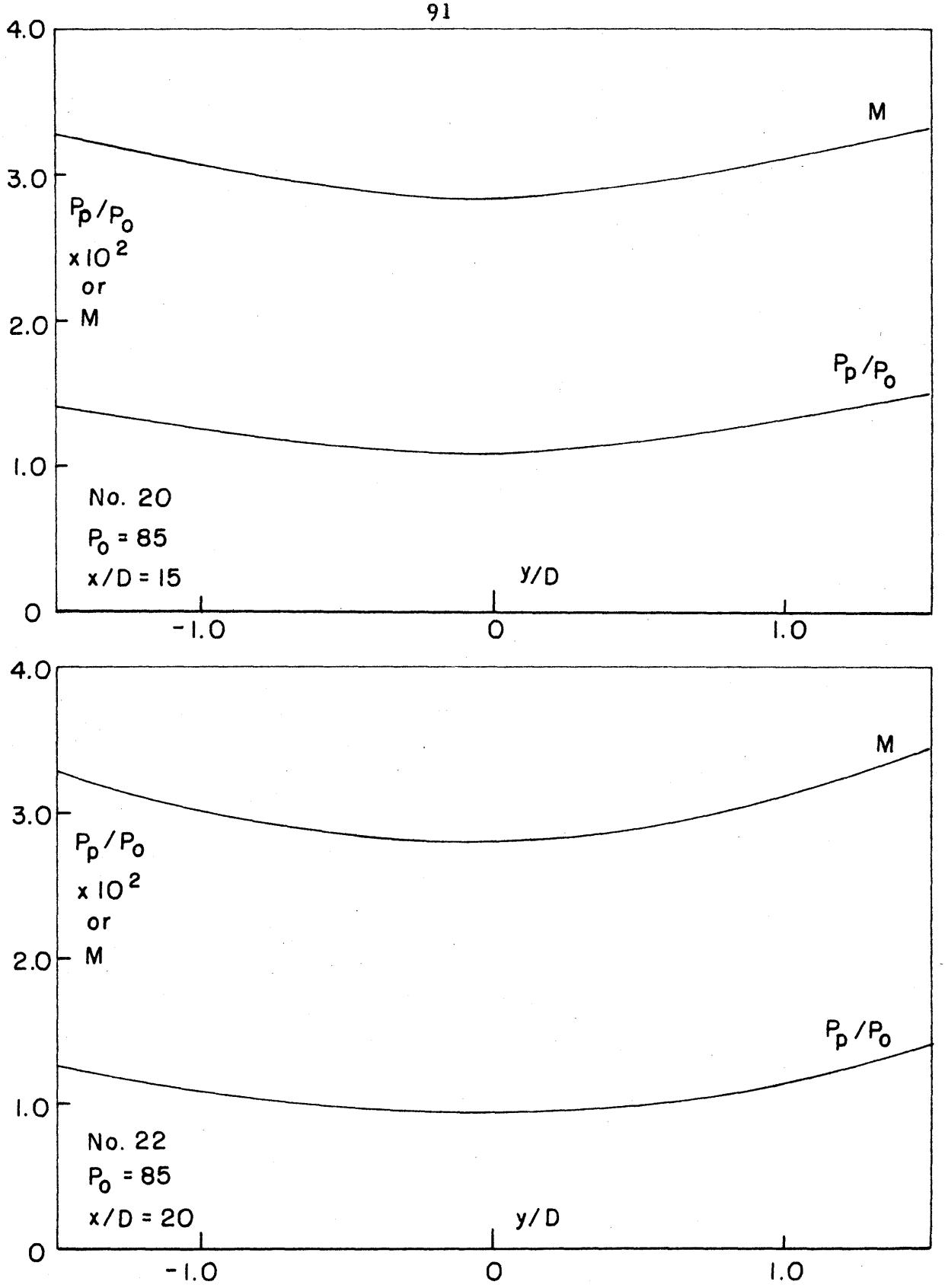

FIG. 20 TOTAL PRESSURE AND MACH TRACES CORRESPONDING TO CONCENTRATION PROFILES, FIG. 10

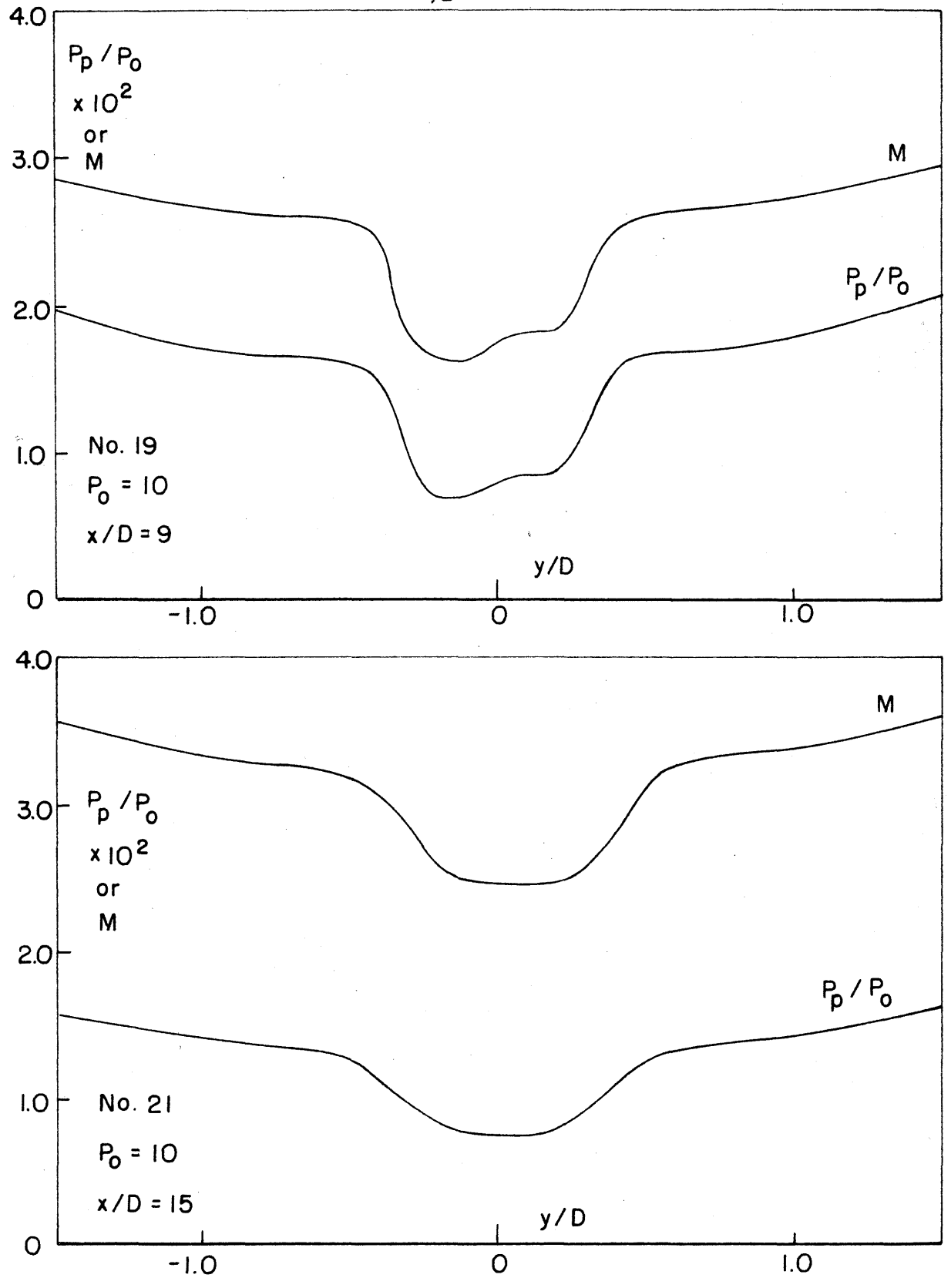

FIG. 21 TOTAL PRESSURE AND MACH TRACES CORRESPONDING TO CONCENTRATION PROFILES, FIG. 11

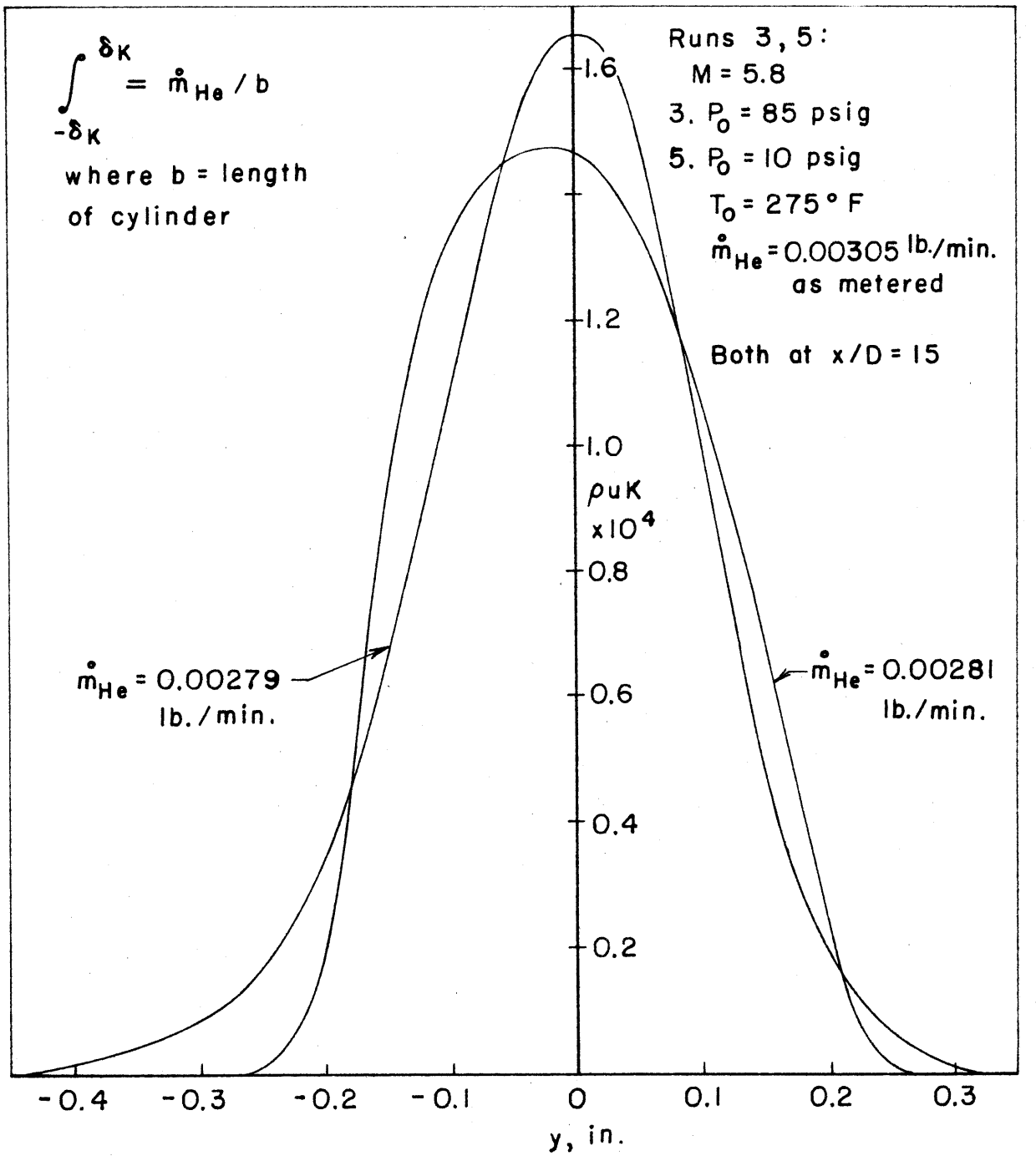

FIG.22 CONTINUITY PROFILE FOR HELIUM MASS PER SECOND IN THE WAKE OF THE POROUS CYLINDER

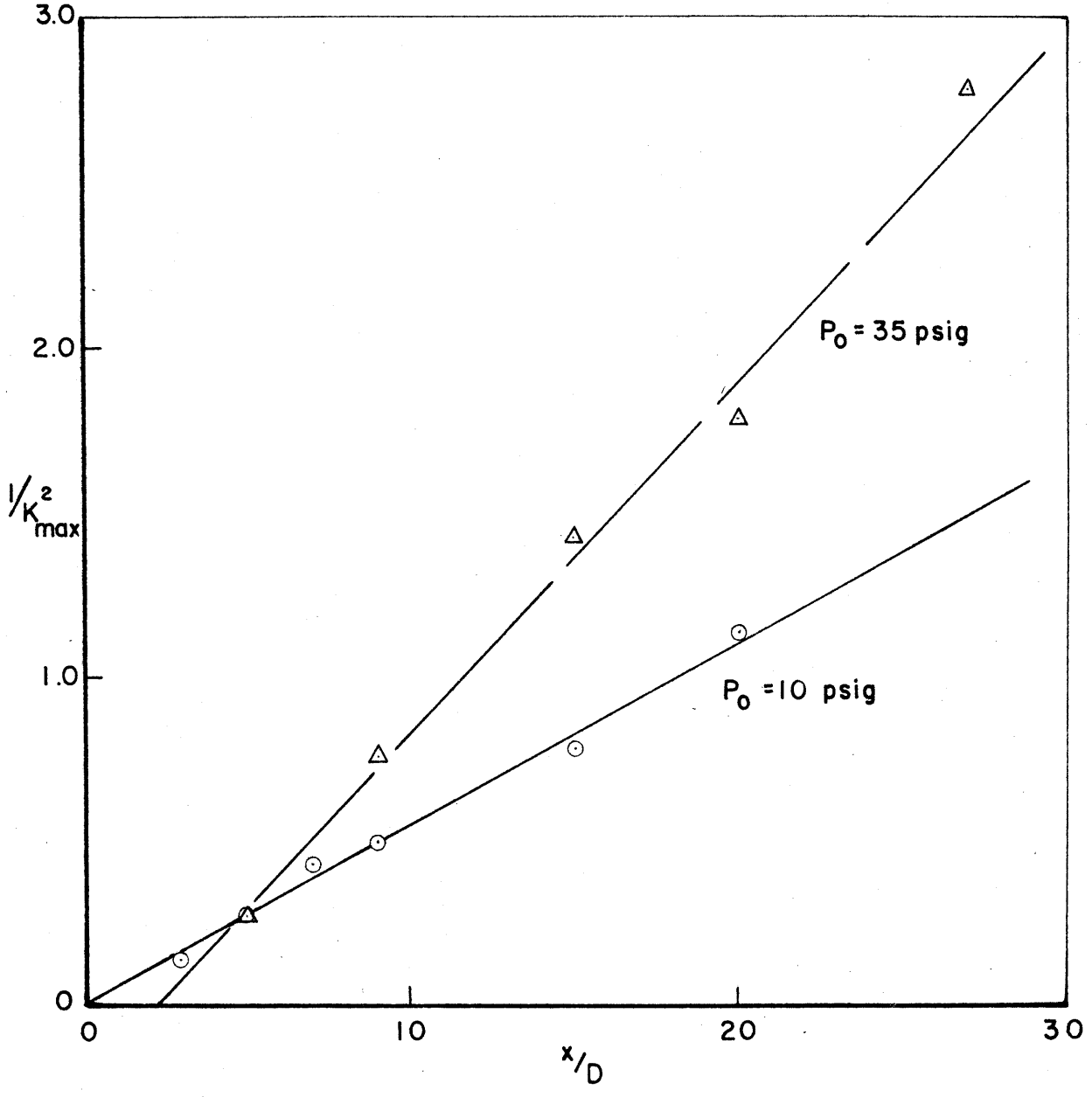

FIG.23 PLOT TO DETERMINE VIRTUAL ORIGIN OF SIMILAR FLOW

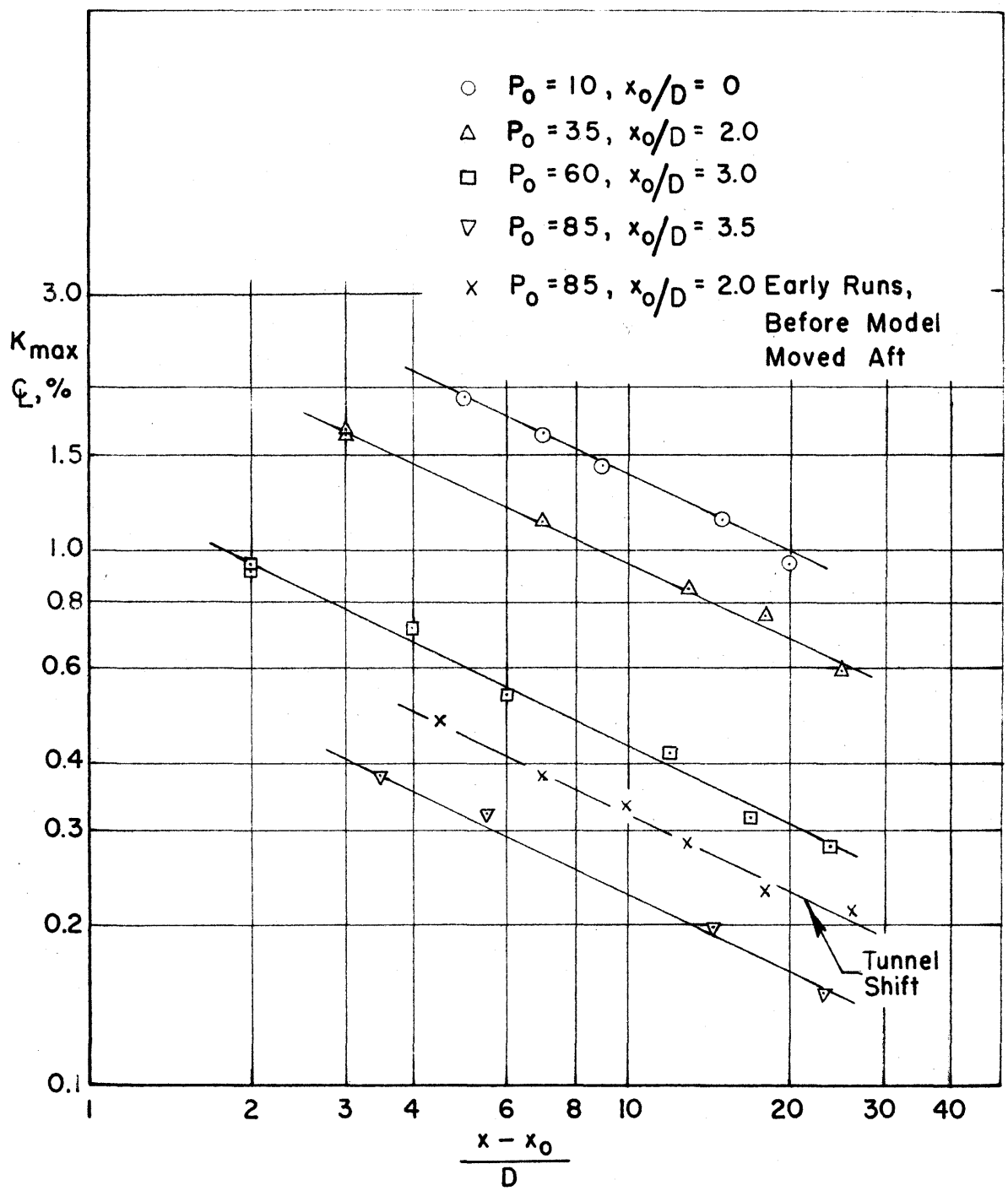

FIG.24 PLOT OF MAXIMUM CONCENTRATION VERSUS AXIAL DISTANCE WITH VIRTUAL ORIGIN CORRECTION

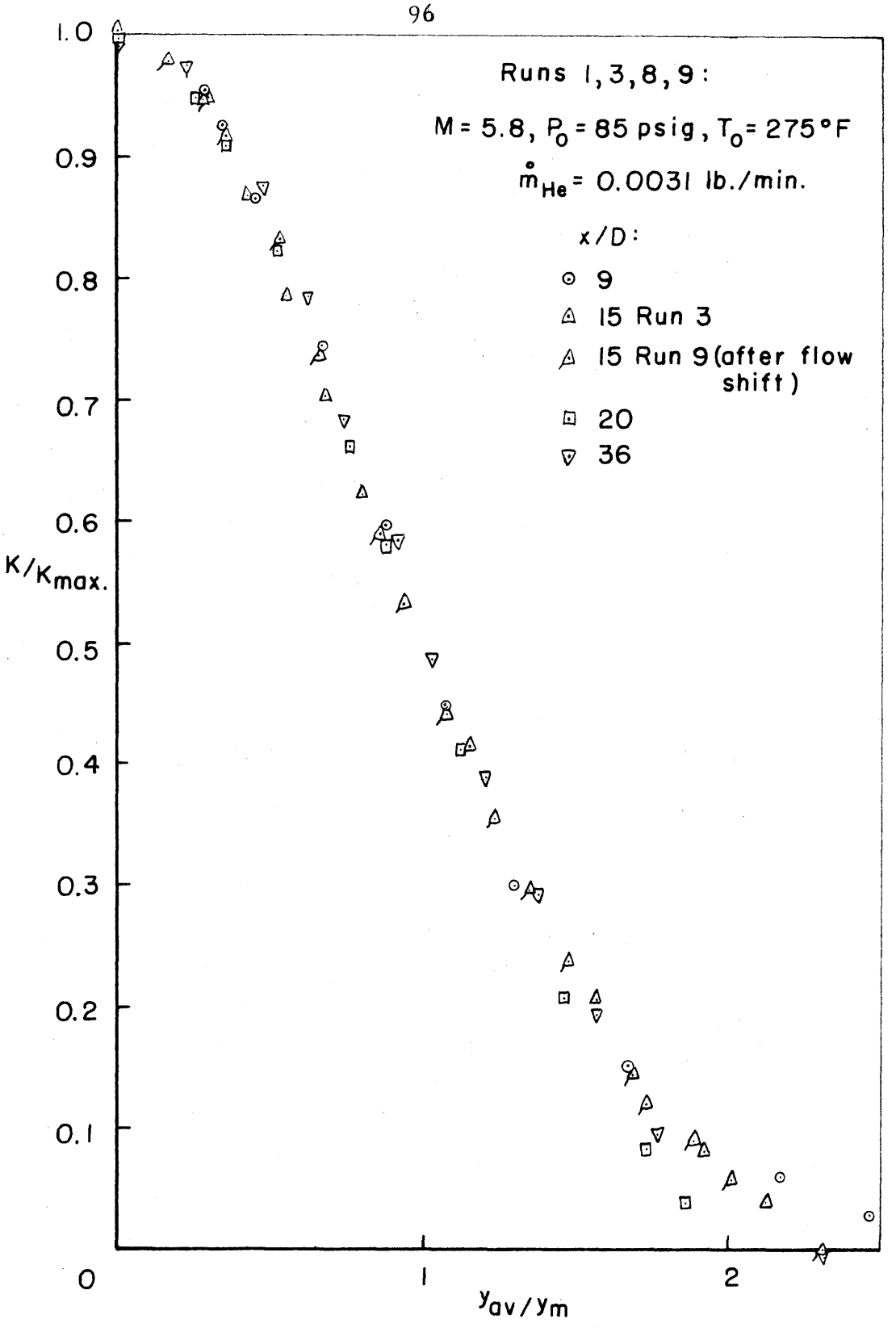

FIG.25 PLOT OF NORMALIZED CONCENTRATION VERSUS AVERAGE NORMALIZED VERTICAL DISTANCE

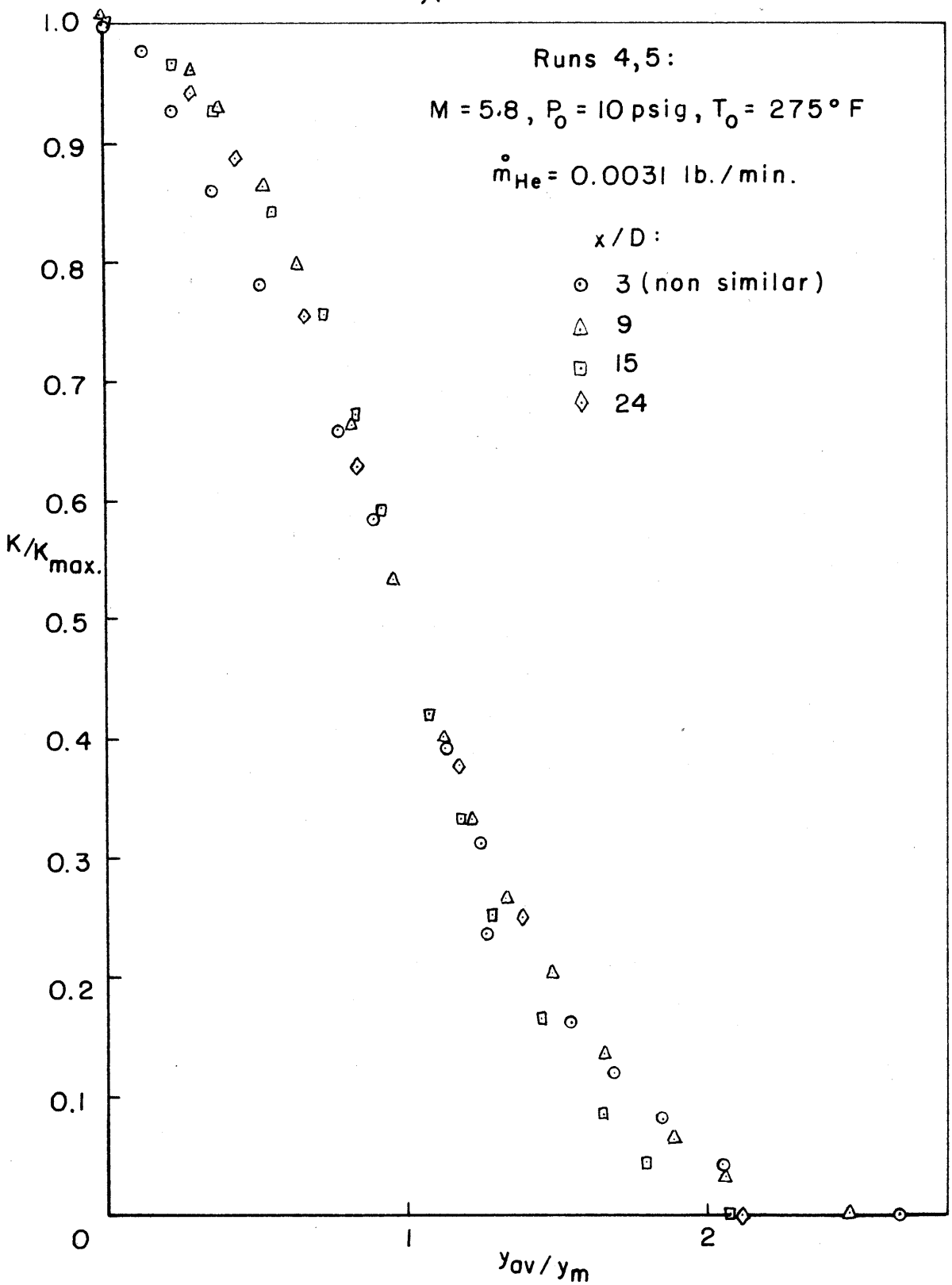

FIG.26 PLOT OF NORMALIZED CONCENTRATION VERSUS AVERAGE NORMALIZED VERTICAL DISTANCE

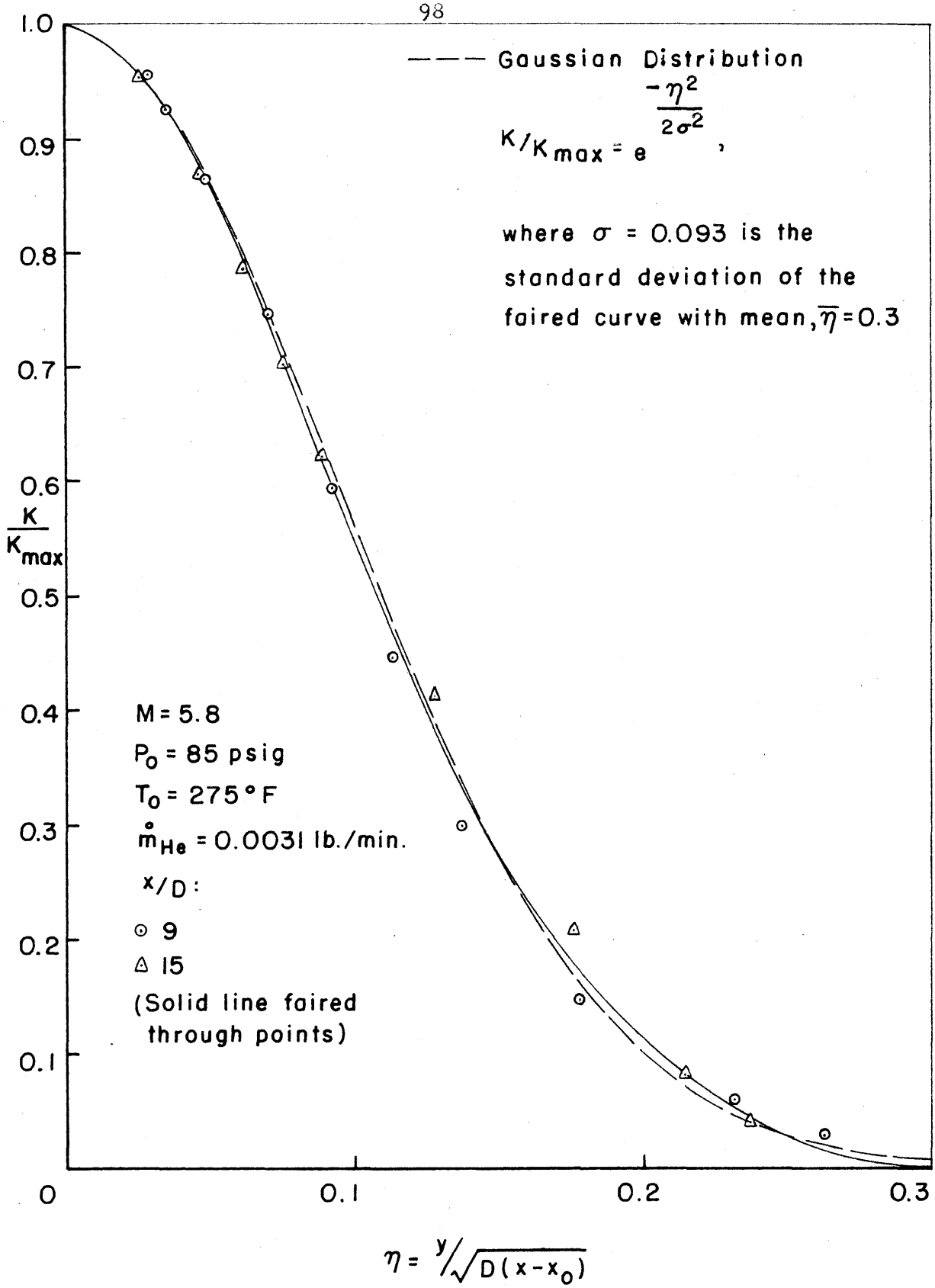

FIG.27 PLOT OF NORMALIZED CONCENTRATION TO SIMILAR COORDINATES VERSUS THE CORRESPONDING GAUSSIAN DISTRIBUTION

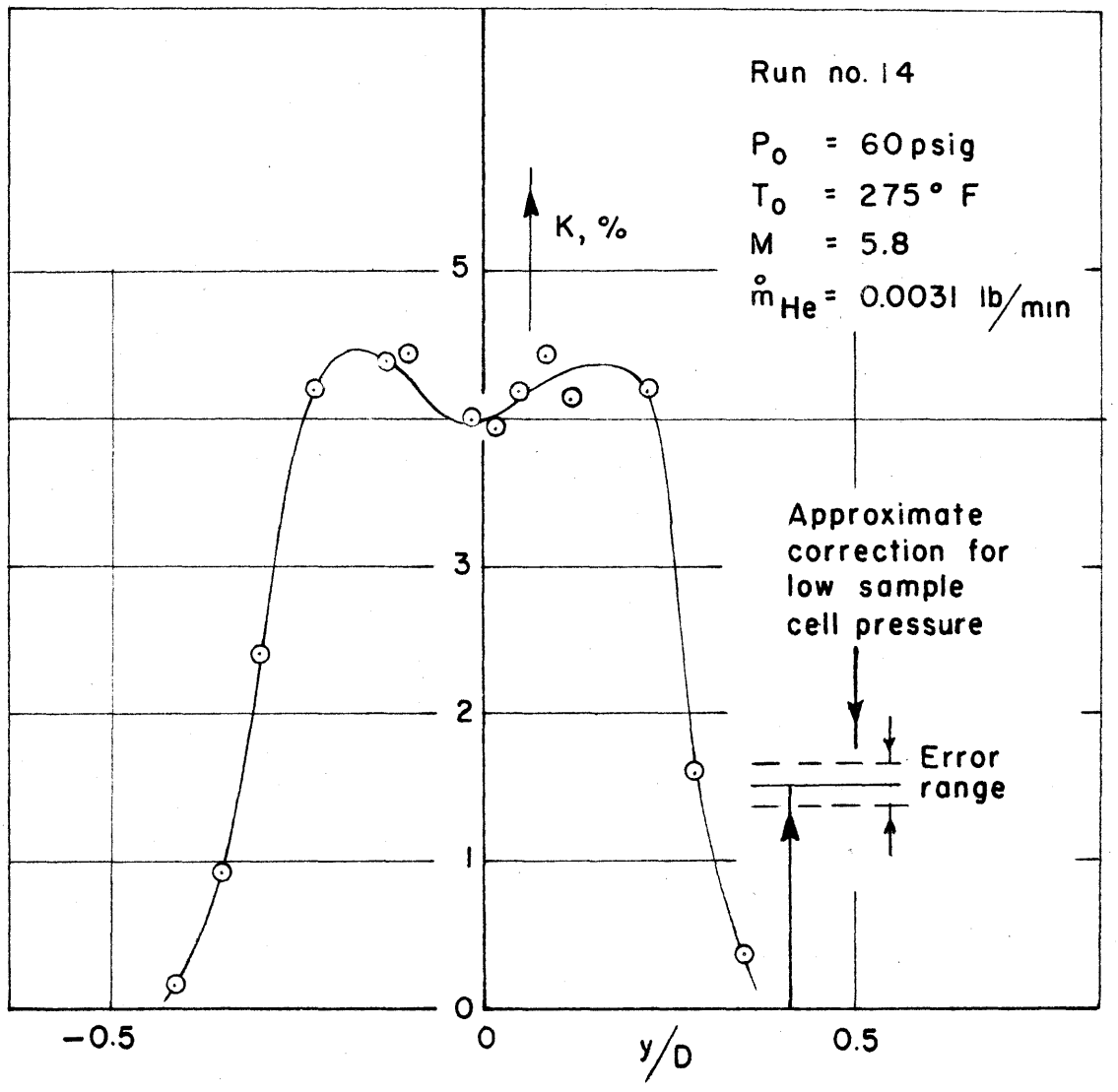

FIG.28 TYPICAL PROFILE IN THE WAKE CAVITY NEAR THE MODEL, $x/D < 2$

APPENDIX

THERMAL CONDUCTIVITY APPARATUS AND PROCEDURE FOR HYPERSONIC WIND TUNNEL EMPLOYMENT

Refer to Figure A-1

I. Preliminary, with probe at desired distance behind model:

1. Check all lines, volumes and valves for leakage.
2. Check concentration measurement on known sample.
3. Start tunnel and stabilize. (Can be done along with 1 and 2.)
4. Make zero concentration check with air in sample and reference cavities. Zero the concentration scale on the recorder. Turn helium on.
5. Prepare to set pressure sensitivity by manually opening valve a, c, and d with m, b, and e closed. Measure total pressure on the micromanometer manually. Close d. Zero the pressure scale on the recorder.
6. Set total pressure sensitivity in recorder ordinate scale; find tunnel centerline by probe movement vertically and set probe position potentiometer to read correctly on abscissa.

II. Measurement of Total Pressure and Concentration:

A. Automatic Operation, where sample is at pitot pressure greater than 1 cm Hg absolute:

1. Set probe vertical distance, valves a, c, e, and f open, and b and d closed. Turn on "washing machine"

type relay system, which follows the following sequence:

(a) Closes valve m and opens n to clear cell - relay holds for sufficient time, then opens m to allow next sample to wash through - relay again holds and then closes m. This operation leaves the cell clean and at low vacuum for drawing of the tunnel sample.

(b) Relay operates after sufficient time to achieve cell vacuum and closes n, then immediately opens m. (With 1 cm Hg or more differential, a tunnel sample is drawn into the cell in satisfactory time for automatic operation.) After sample is drawn, relays switch to transducer circuit and drop recorder pen momentarily for total pressure, then switching to cell bridge circuit, drop pen for concentration.

(c) Relay cycle is complete. Move probe and repeat for other points. This procedure obtains both total pressure and concentration.

B. Manual Operation, where sample is at pitot pressure less than 1 cm Hg absolute:

The pressure correction in this range is too great for direct concentration measurement of the sample at pitot pressure. The sample must be compressed. The hand-operated pump is adequate in that very few readings are

taken at these low pressures with the present tunnel densities. The mercury pump itself may be designed as a micromanometer, in which case it may be used for the reading of cell pressures and will be more convenient for the manual operation than the transducer. (For a description of the hand operation, see Sections II. 7. 1. and III. 5. of the basic report.)

The measurement of total pressure along with compressed sample pressure requires additional steps. Usually, however, it will not be necessary to obtain total pressure at these low sample pressures, as they occur only in non-similar regions near the model.

If possible, the cell bridge current should be turned off during each interval when the cell is completely evacuated. (See Section II. 7. 1. of the basic report.)

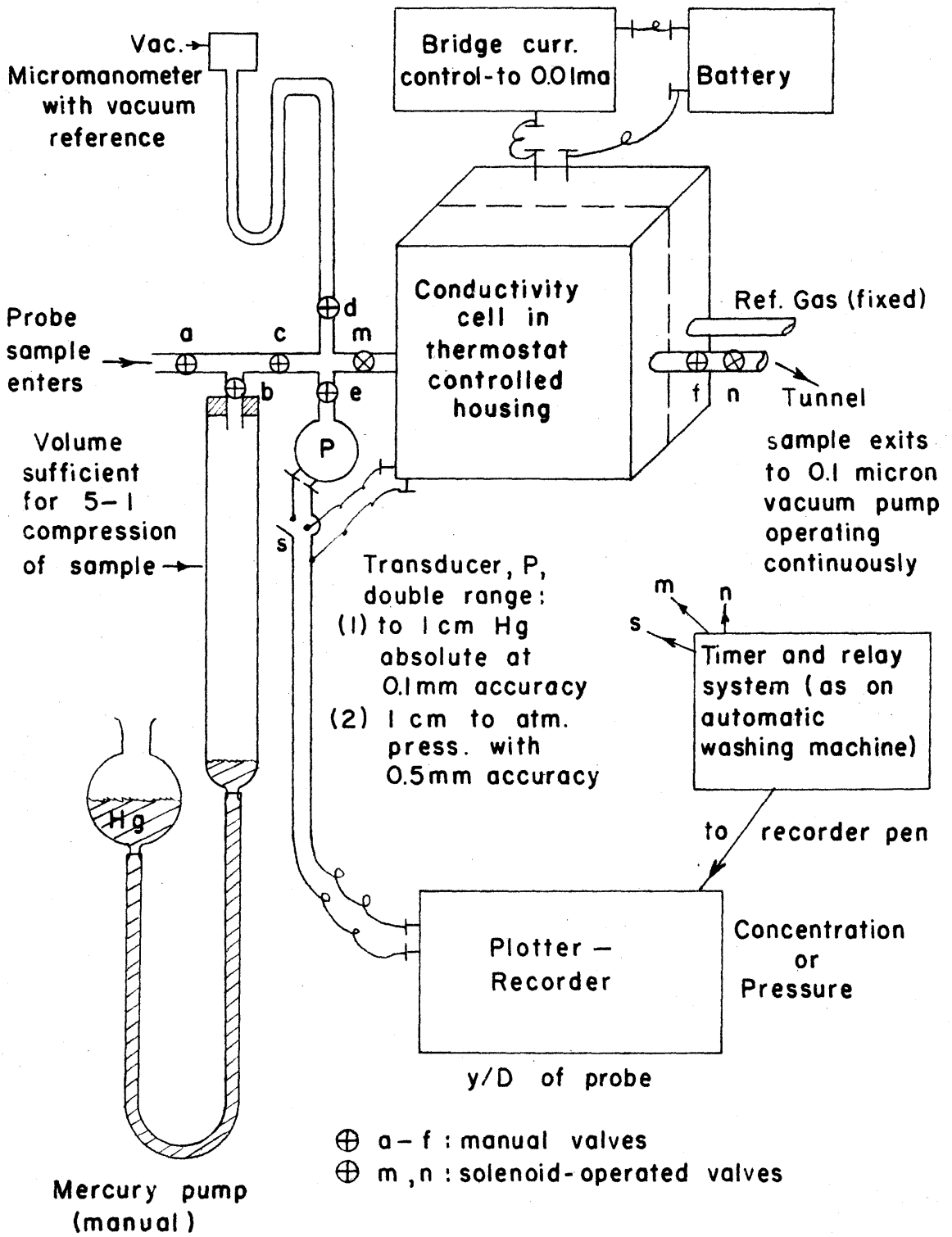

FIG. A-1: SCHEMATIC OF A SYSTEM TO MEASURE CONCENTRATION AND TOTAL PRESSURE AT LOW SAMPLE DENSITIES